arXiv:hep-ph/0306306v2 3 Oct 2003

HU-EP-03/35

Weak decays of the B_c meson to charmonium and D mesons in the relativistic quark model

D. Ebert

Institut für Physik, Humboldt–Universität zu Berlin, Newtonstr. 15, D-12489 Berlin, Germany

R. N. Faustov and V. O. Galkin

Institut für Physik, Humboldt–Universität zu Berlin, Newtonstr. 15, D-12489 Berlin, Germany and

Russian Academy of Sciences, Scientific Council for Cybernetics, Vavilov Street 40, Moscow 117333, Russia

Semileptonic and nonleptonic decays of the B_c meson to charmonium and D mesons are studied in the framework of the relativistic quark model. The decay form factors are explicitly expressed through the overlap integrals of the meson wave functions in the whole accessible kinematical range. The relativistic meson wave functions are used for the calculation of the decay rates. The obtained results are compared with the predictions of other approaches.

PACS numbers: 13.20.He, 12.39.Ki, 14.40.Nd

I. INTRODUCTION

The investigation of weak decays of mesons composed of a heavy quark and antiquark gives a very important insight in the heavy quark dynamics. The properties of the B_c meson are of special interest, since it is the only heavy meson consisting of two heavy quarks with different flavor. This difference of quark flavors forbids annihilation into gluons. As a result, the excited B_c meson states lying below the BD production threshold undergo pionic or radiative transitions to the pseudoscalar ground state which is considerably more stable than corresponding charmonium or bottomonium states and decays only weakly. The Collider Detector at Fermilab (CDF) Collaboration [1] reported the discovery of the B_c ground state in $p\bar{p}$ collisions. More experimental data are expected to come in near future from the Tevatron and Large Hadron Collider (LHC).

The characteristic feature of the B_c meson is that both quarks forming it are heavy and thus their weak decays give comparable contributions to the total decay rate. Therefore it is necessary to consider both the b quark decays $b \to c, u$ with the $\bar{c}$ quark being a spectator and $\bar{c}$ quark decays $\bar{c} \to \bar{s}, \bar{d}$ with b quark being a spectator. The former transitions lead to semileptonic decays to charmonium and D mesons while the latter lead to decays to B_s and B mesons. The estimates of the B_c decay rates indicate that the c quark decays give the dominant contribution ($\sim 70\%$) while the b quark decays and weak annihilation contribute about 20% and 10%, respectively (for a recent review see e.g. [2] and references

therein). However, from the experimental point of view the B_c decays to charmonium are easier to identify. Indeed, CDF observed B_c mesons [1] analysing their semileptonic decays $B_c \to J/\psi l\nu$.

The important difference between the B_c semileptonic decays induced by $b \to c, u$ and $c \to s, d$ transitions lies in the substantial difference of their kinematical ranges. In the case of B_c decays to charmonium and $D^{(*)}$ mesons the kinematical range (the square of momentum transfer to the lepton pair varies from 0 to $q^2_{\rm max} \approx 10$ GeV^2 for decays to J/ψ and $q^2_{\rm max} \approx 18$ GeV^2 for decays to D mesons) is considerably broader than for decays to $B_s^{(*)}$ and $B^{(*)}$ mesons ($q^2_{\rm max} \approx 0.8$ GeV^2 for decays to B_s and $q^2_{\rm max} \approx 1$ GeV^2 for decays to B mesons). As a result in the B_c meson rest frame the maximum recoil momentum of the final charmonium and D mesons is of the same order of magnitude as their masses, while the maximum recoil momentum of the $B_s^{(*)}$ and $B^{(*)}$ mesons is considerably smaller than the meson masses. This significant difference in kinematics makes it reasonable to consider B_c decays induced by b and c quark decays separately.

In this paper we consider weak B_c decays to charmonium and D mesons in the framework of the relativistic quark model based on the quasipotential approach in quantum field theory. This model has been successfully applied for the calculations of mass spectra, radiative and weak decays of heavy quarkonia and heavy-light mesons [3–8]. In our recent paper [9] we applied this model for the investigation of properties of the B_c meson and heavy quarkonia. The relativistic wave functions obtained there are used for the calculation of the transition matrix elements. The consistent theoretical description of B_c decays to charmonium and D mesons requires a reliable determination of the q^2 dependence of the decay amplitudes in the whole kinematical range. In most previous calculations the corresponding decay form factors were determined only at one kinematical point either $q^2 = 0$ or $q^2 = q^2_{\rm max}$ and then extrapolated to the allowed kinematical range using some phenomenological ansatz (mainly (di)pole or Gaussian). Our aim is to explicitly determine the q^2 dependence of form factors in the whole kinematical range in order to avoid extrapolations thus reducing uncertainties. The large values of recoil momentum require the consistent relativistic treatment of these decays. In particular, the relativistic transformation of the meson wave functions from the moving to the rest reference frame should be taken into account. On the other hand, the presence of only heavy quarks in B_c and charmonium allows one to use expansions in the inverse powers of heavy quark masses $1/m_{b,c}$.

The paper is organized as follows. In Sec. II we describe the underlying relativistic quark model. The method for calculating matrix elements of the weak current for $b \to c, u$ transitions in B_c meson decays is presented in Sec. III. Special attention is devoted to the dependence of the decay amplitudes on the momentum transfer. The B_c decay form factors are calculated in the whole kinematical range in Sec. IV. The q^2 dependence of the form factors is explicitly determined. These form factors are used for the calculation of the B_c semileptonic decay rates in Sec. V. Section VI contains our predictions for the energetic nonleptonic B_c decays in the factorization approximation, and a comparison of our results with other theoretical calculations is presented. Our conclusions are given in Sec. VII. Finally, the Appendix contains complete expressions for the decay form factors.

II. RELATIVISTIC QUARK MODEL

In the quasipotential approach a meson is described by the wave function of the bound quark-antiquark state, which satisfies the quasipotential equation [10] of the Schrödinger

type [11]

$$\left(\frac{b^2(M)}{2\mu_R}-\frac{\mathbf{p}^2}{2\mu_R}\right)\Psi_M(\mathbf{p})=\int\frac{d^3q}{(2\pi)^3}V(\mathbf{p},\mathbf{q};M)\Psi_M(\mathbf{q}), \tag{1}$$

where the relativistic reduced mass is

$$\mu_R=\frac{E_1E_2}{E_1+E_2}=\frac{M^4-(m_1^2-m_2^2)^2}{4M^3}, \tag{2}$$

and E_1, E_2 are the center of mass energies on mass shell given by

$$E_1=\frac{M^2-m_2^2+m_1^2}{2M},\quad E_2=\frac{M^2-m_1^2+m_2^2}{2M}. \tag{3}$$

Here $M=E_1+E_2$ is the meson mass, $m_{1,2}$ are the quark masses, and $\mathbf{p}$ is their relative momentum. In the center of mass system the relative momentum squared on mass shell reads

$$b^2(M)=\frac{[M^2-(m_1+m_2)^2][M^2-(m_1-m_2)^2]}{4M^2}. \tag{4}$$

The kernel $V(\mathbf{p},\mathbf{q};M)$ in Eq. (1) is the quasipotential operator of the quark-antiquark interaction. It is constructed with the help of the off-mass-shell scattering amplitude, projected onto the positive energy states. Constructing the quasipotential of the quark-antiquark interaction, we have assumed that the effective interaction is the sum of the usual one-gluon exchange term with the mixture of long-range vector and scalar linear confining potentials, where the vector confining potential contains the Pauli interaction. The quasipotential is then defined by [3]

$$V(\mathbf{p},\mathbf{q};M)=\bar{u}_1(p)\bar{u}_2(-p)\mathcal{V}(\mathbf{p},\mathbf{q};M)u_1(q)u_2(-q), \tag{5}$$

with

$$\mathcal{V}(\mathbf{p},\mathbf{q};M)=\frac{4}{3}\alpha_sD_{\mu\nu}(\mathbf{k})\gamma_1^\mu\gamma_2^\nu+V_{\rm conf}^V(\mathbf{k})\Gamma_1^\mu\Gamma_{2;\mu}+V_{\rm conf}^S(\mathbf{k}),$$

where α_s is the QCD coupling constant, $D_{\mu\nu}$ is the gluon propagator in the Coulomb gauge

$$D^{00}(\mathbf{k})=-\frac{4\pi}{\mathbf{k}^2},\quad D^{ij}(\mathbf{k})=-\frac{4\pi}{k^2}\left(\delta^{ij}-\frac{k^ik^j}{\mathbf{k}^2}\right),\quad D^{0i}=D^{i0}=0, \tag{6}$$

and $\mathbf{k}=\mathbf{p}-\mathbf{q}$; γ_μ and $u(p)$ are the Dirac matrices and spinors

$$u^\lambda(p)=\sqrt{\frac{\epsilon(p)+m}{2\epsilon(p)}}\begin{pmatrix}1\\ \dfrac{\boldsymbol{\sigma}\mathbf{p}}{\epsilon(p)+m}\end{pmatrix}\chi^\lambda. \tag{7}$$

Here $\boldsymbol{\sigma}$ and χ^λ are the Pauli matrices and spinors; $\epsilon(p)=\sqrt{p^2+m^2}$. The effective long-range vector vertex is given by

$$\Gamma_\mu(\mathbf{k})=\gamma_\mu+\frac{i\kappa}{2m}\sigma_{\mu\nu}k^\nu, \tag{8}$$

where κ is the Pauli interaction constant characterizing the long-range anomalous chromomagnetic moment of quarks. Vector and scalar confining potentials in the nonrelativistic limit reduce to

$$\begin{aligned}V_V(r)&=(1-\varepsilon)Ar+B,\\ V_S(r)&=\varepsilon Ar,\end{aligned} \tag{9}$$

reproducing

$$V_{\rm conf}(r) = V_S(r) + V_V(r) = Ar + B, \tag{10}$$

where ε is the mixing coefficient.

The expression for the quasipotential of the heavy quarkonia, expanded in v^2/c^2 without and with retardation corrections to the confining potential, can be found in Refs. [3] and [4, 9], respectively. The structure of the spin-dependent interaction is in agreement with the parameterization of Eichten and Feinberg [12]. The quasipotential for the heavy quark interaction with a light antiquark without employing the expansion in inverse powers of the light quark mass is given in Ref. [5]. All the parameters of our model like quark masses, parameters of the linear confining potential A and B, mixing coefficient ε and anomalous chromomagnetic quark moment κ are fixed from the analysis of heavy quarkonium masses [3] and radiative decays [6]. The quark masses $m_b = 4.88$ GeV, $m_c = 1.55$ GeV, $m_{u,d} = 0.33$ GeV and the parameters of the linear potential $A = 0.18$ GeV^2 and $B = -0.16$ GeV have usual values of quark models. The value of the mixing coefficient of vector and scalar confining potentials $\varepsilon = -1$ has been determined from the consideration of the heavy quark expansion for the semileptonic $B \to D$ decays [7] and charmonium radiative decays [6]. Finally, the universal Pauli interaction constant $\kappa = -1$ has been fixed from the analysis of the fine splitting of heavy quarkonia ^3P_J- states [3]. Note that the long-range magnetic contribution to the potential in our model is proportional to $(1 + \kappa)$ and thus vanishes for the chosen value of $\kappa = -1$. It has been known for a long time that the correct reproduction of the spin-dependent part of the quark-antiquark interaction requires either assuming the scalar confinement or equivalently introducing the Pauli interaction with $\kappa = -1$ [3, 4, 13] in the vector confinement.

III. MATRIX ELEMENTS OF THE ELECTROWEAK CURRENT FOR $b \to c, u$ TRANSITIONS

In order to calculate the exclusive semileptonic decay rate of the B_c meson, it is necessary to determine the corresponding matrix element of the weak current between meson states. In the quasipotential approach, the matrix element of the weak current $J^W_\mu = \bar{q}\gamma_\mu(1-\gamma_5)b$, associated with $b \to q$ ($q = c$ or u) transition, between a B_c meson with mass M_{B_c} and momentum p_{B_c} and a final meson F ($F = \psi, \eta_c$ or $D^{(*)}$) with mass M_F and momentum p_F takes the form [14]

$$\langle F(p_F)|J^W_\mu|B_c(p_{B_c})\rangle = \int \frac{d^3p\, d^3q}{(2\pi)^6} \bar{\Psi}_{F\,\mathbf{p}_F}(\mathbf{p})\Gamma_\mu(\mathbf{p},\mathbf{q})\Psi_{B_c\,\mathbf{p}_{B_c}}(\mathbf{q}), \tag{11}$$

where $\Gamma_\mu(\mathbf{p},\mathbf{q})$ is the two-particle vertex function and $\Psi_{M\,\mathbf{p}_M}$ are the meson ($M = B_c, F$) wave functions projected onto the positive energy states of quarks and boosted to the moving reference frame with momentum $\mathbf{p}_M$.

The contributions to Γ come from Figs. 1 and 2. The contribution $\Gamma^{(2)}$ is the consequence of the projection onto the positive-energy states. Note that the form of the relativistic corrections resulting from the vertex function $\Gamma^{(2)}$ is explicitly dependent on the Lorentz structure of the quark-antiquark interaction. In the leading order of the v^2/c^2 expansion for B_c and ψ and in the heavy quark limit $m_c \to \infty$ for D only $\Gamma^{(1)}$ contributes, while $\Gamma^{(2)}$ contributes already at the subleading order. The vertex functions look like

$$\Gamma^{(1)}_\mu(\mathbf{p},\mathbf{q}) = \bar{u}_q(p_q)\gamma_\mu(1-\gamma^5)u_b(q_b)(2\pi)^3\delta(\mathbf{p}_c - \mathbf{q}_c), \tag{12}$$

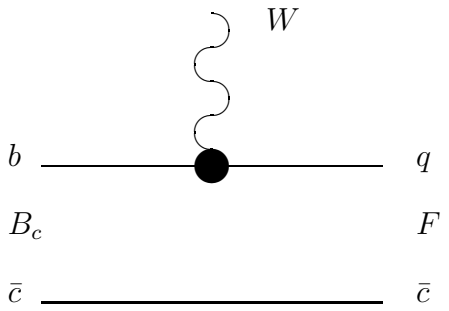

FIG. 1: Lowest order vertex function $\Gamma^{(1)}$ contributing to the current matrix element (11).

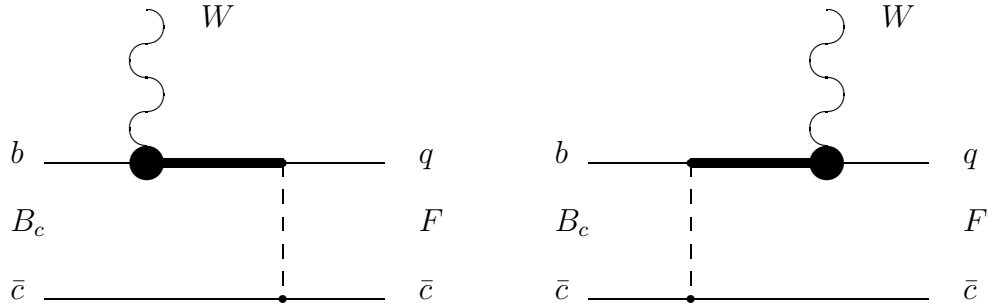

FIG. 2: Vertex function $\Gamma^{(2)}$ taking the quark interaction into account. Dashed lines correspond to the effective potential $\mathcal{V}$ in (5). Bold lines denote the negative-energy part of the quark propagator.

and

$$\Gamma^{(2)}_{\mu}(\mathbf{p},\mathbf{q}) \;=\; \bar{u}_q(p_q)\bar{u}_c(p_c)\Big\{\gamma_{1\mu}(1-\gamma_1^5)\frac{\Lambda_b^{(-)}(k)}{\epsilon_b(k)+\epsilon_b(p_q)}\gamma_1^0\mathcal{V}(\mathbf{p}_c-\mathbf{q}_c) + \mathcal{V}(\mathbf{p}_c-\mathbf{q}_c)\frac{\Lambda_q^{(-)}(k')}{\epsilon_q(k')+\epsilon_q(q_b)}\gamma_1^0\gamma_{1\mu}(1-\gamma_1^5)\Big\}u_b(q_b)u_c(q_c), \tag{13}$$

where the superscripts "(1)" and "(2)" correspond to Figs. 1 and 2, $\mathbf{k}=\mathbf{p}_q-\mathbf{\Delta}$; $\mathbf{k}'=\mathbf{q}_b+\mathbf{\Delta}$; $\mathbf{\Delta}=\mathbf{p}_F-\mathbf{p}_{B_c}$;

$$\Lambda^{(-)}(p)=\frac{\epsilon(p)-(m\gamma^0+\gamma^0(\boldsymbol{\gamma}\mathbf{p}))}{2\epsilon(p)}.$$

Here [14]

$$p_{q,c} \;=\; \epsilon_{q,c}(p)\frac{p_F}{M_F}\pm\sum_{i=1}^{3}n^{(i)}(p_F)p^i,$$

$$q_{b,c} \;=\; \epsilon_{b,c}(q)\frac{p_{B_c}}{M_{B_c}}\pm\sum_{i=1}^{3}n^{(i)}(p_{B_c})q^i,$$

and $n^{(i)}$ are three four-vectors given by

$$n^{(i)\mu}(p)=\left\{\frac{p^i}{M},\;\delta_{ij}+\frac{p^ip^j}{M(E+M)}\right\},\quad E=\sqrt{\mathbf{p}^2+M^2}.$$

It is important to note that the wave functions entering the weak current matrix element (11) are not in the rest frame in general. For example, in the B_c meson rest frame ($\mathbf{p}_{B_c}=0$), the final meson is moving with the recoil momentum $\mathbf{\Delta}$. The wave function of the moving meson $\Psi_{F\,\mathbf{\Delta}}$ is connected with the wave function in the rest frame $\Psi_{F\,\mathbf{0}} \equiv \Psi_F$ by the transformation [14]

$$\Psi_{F\,\mathbf{\Delta}}(\mathbf{p}) = D_q^{1/2}(R^W_{L_{\mathbf{\Delta}}}) D_c^{1/2}(R^W_{L_{\mathbf{\Delta}}}) \Psi_{F\,\mathbf{0}}(\mathbf{p}), \tag{14}$$

where R^W is the Wigner rotation, $L_{\mathbf{\Delta}}$ is the Lorentz boost from the meson rest frame to a moving one, and the rotation matrix $D^{1/2}(R)$ in spinor representation is given by

$$\begin{pmatrix} 1 & 0 \\ 0 & 1 \end{pmatrix} D^{1/2}_{q,c}(R^W_{L_{\mathbf{\Delta}}}) = S^{-1}(\mathbf{p}_{q,c}) S(\mathbf{\Delta}) S(\mathbf{p}), \tag{15}$$

where

$$S(\mathbf{p}) = \sqrt{\frac{\epsilon(p)+m}{2m}} \left(1 + \frac{\boldsymbol{\alpha}\mathbf{p}}{\epsilon(p)+m} \right)$$

is the usual Lorentz transformation matrix of the four-spinor.

The general structure of the current matrix element (11) is rather complicated, because it is necessary to integrate both with respect to d^3p and d^3q. The δ-function in the expression (12) for the vertex function $\Gamma^{(1)}$ permits to perform one of these integrations. As a result the contribution of $\Gamma^{(1)}$ to the current matrix element has the usual structure of an overlap integral of meson wave functions and can be calculated exactly (without employing any expansion) in the whole kinematical range, if the wave functions of the initial and final meson are known. The situation with the contribution $\Gamma^{(2)}$ is different. Here, instead of a δ-function, we have a complicated structure, containing the potential of the $q\bar{q}$-interaction in meson. Thus in the general case we cannot get rid of one of the integrations in the contribution of $\Gamma^{(2)}$ to the matrix element (11). Therefore, it is necessary to use some additional considerations in order to simplify calculations. The main idea is to expand the vertex function $\Gamma^{(2)}$, given by (13), in such a way that it will be possible to use the quasipotential equation (1) in order to perform one of the integrations in the current matrix element (11).

***$B_c \to \psi, \eta_c$* transitions.** The natural expansion parameters for B_c decays to charmonium are the active heavy b and c quark masses as well as the spectator c quark mass. We carry such an expansion up to the second order in the ratios of the relative quark momentum $\mathbf{p}$ and binding energy to the heavy quark masses $m_{b,c}$. It is important to take into account the fact that in the case of weak B_c decays caused by $b \to c, u$ quark transition the kinematically allowed range is large ($|\mathbf{\Delta}_{\max}| = (M^2_{B_c} - M^2_F)/(2M_{B_c}) \sim 2.4$ GeV for decays to charmonium and ~ 2.8 GeV for decays to D mesons). This means that the recoil momentum $\mathbf{\Delta}$ of a final meson is large in comparison to the relative momentum $\mathbf{p}$ of quarks inside a meson (~ 0.5 GeV), being of the same order as the heavy quark mass almost in the whole kinematical range. Thus we do not use expansions in powers of $|\mathbf{\Delta}|/m_{b,c}$ or $|\mathbf{\Delta}|/M_F$, but approximate in the expression (13) for $\Gamma^{(2)}$ the heavy quark energies $\epsilon_{b,c}(p+\Delta) \equiv \sqrt{m^2_{b,c} + (\mathbf{p}+\mathbf{\Delta})^2}$ by $\epsilon_{b,c}(\Delta) \equiv \sqrt{m^2_{b,c} + \mathbf{\Delta}^2}$, which become independent of the quark relative momentum $\mathbf{p}$. Making these replacements and expansions we see that it is possible to integrate the current matrix element (11) either with respect to d^3p or d^3q using the quasipotential equation (1). Performing integrations and taking the sum of the contributions of $\Gamma^{(1)}$ and $\Gamma^{(2)}$ we get the expression for the current matrix element, which contains ordinary overlap integrals of

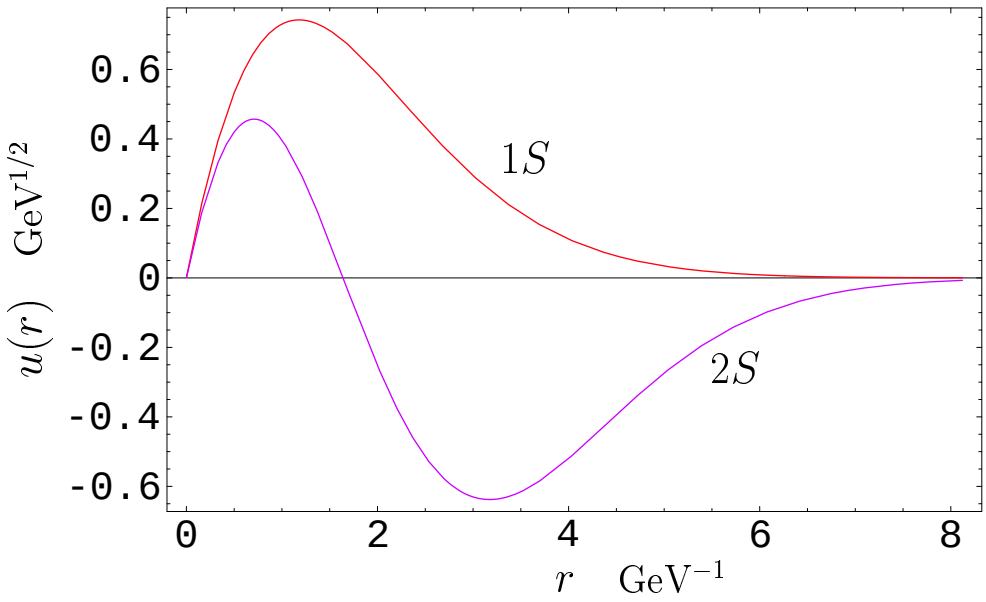

FIG. 3: The reduced radial wave functions for the S-states of the B_c meson.

meson wave functions and is valid in the whole kinematical range. Thus this matrix element can be easily calculated using numerical wave functions found in our meson mass spectrum analysis [4, 9]. The reduced radial wave functions $u(r) \equiv rR(r)$ of the B_c meson are shown in Fig. 3.

$B_c \to D^{(*)}$ transitions. In this case the heavy b quark undergoes the weak transition to the light u quark. The constituent u quark mass is of the same order of magnitude as the relative momentum and binding energy, thus we cannot apply the expansion in inverse powers of its mass. Nevertheless, taking into account the fact that the recoil momentum of the final meson in this decay is large almost in the whole kinematical range (as it was discussed above), we can neglect the relative momentum $\mathbf{p}$ of quarks inside a meson with respect to the large recoil momentum $\mathbf{\Delta}$. Thus in the region of large recoil ($|\mathbf{\Delta}| \gg |\mathbf{p}|$) we can use the same expressions of the $\Gamma^{(2)}$ contribution to the current matrix element both for the $B_c \to D^{(*)}$ and $B_c \to \psi, \eta_c$ transitions. Moreover, the smallness of the $\Gamma^{(2)}$ contribution, which is proportional to the small binding energy, and its weak dependence on momentum transfer allows one to extrapolate these formulae to the whole kinematical range. As numerical estimates show (see below), such extrapolation introduces only small uncertainties.

IV. B_c DECAY FORM FACTORS

The matrix elements of the weak current J^W for B_c decays to pseudoscalar mesons ($P = \eta_c, D$) can be parametrized by two invariant form factors:

$$\langle P(p_F)|\bar{q}\gamma^\mu b|B_c(p_{B_c})\rangle = f_+(q^2)\left[p^\mu_{B_c} + p^\mu_F - \frac{M^2_{B_c} - M^2_P}{q^2}\, q^\mu\right] + f_0(q^2)\frac{M^2_{B_c} - M^2_P}{q^2}\, q^\mu, \quad (16)$$

where $q = p_{B_c} - p_F$; M_{B_c} is the B_c meson mass and M_P is the pseudoscalar meson mass.

The corresponding matrix elements for B_c decays to vector mesons ($V = J/\psi, D^*$) are parametrized by four form factors

$$\langle V(p_F)|\bar{q}\gamma^\mu b|B(p_{B_c})\rangle = \frac{2iV(q^2)}{M_{B_c}+M_V}\epsilon^{\mu\nu\rho\sigma}\epsilon^*_\nu p_{B_c\rho}p_{F\sigma}, \tag{17}$$

$$\begin{aligned}\langle V(p_F)|\bar{q}\gamma^\mu\gamma_5 b|B(p_{B_c})\rangle &= 2M_V A_0(q^2)\frac{\epsilon^*\cdot q}{q^2}\,q^\mu + (M_{B_c}+M_V)A_1(q^2)\left(\epsilon^{*\mu} - \frac{\epsilon^*\cdot q}{q^2}\,q^\mu\right)\\ &\quad -A_2(q^2)\frac{\epsilon^*\cdot q}{M_{B_c}+M_V}\left[p^\mu_{B_c}+p^\mu_F - \frac{M^2_{B_c}-M^2_V}{q^2}\,q^\mu\right],\end{aligned} \tag{18}$$

where M_V and ϵ_μ are the mass and polarization vector of the final vector meson. The following relations hold for the form factors at the maximum recoil point of the final meson ($q^2 = 0$)

$$f_+(0) = f_0(0),$$
$$A_0(0) = \frac{M_{B_c}+M_V}{2M_V}A_1(0) - \frac{M_{B_c}-M_V}{2M_V}A_2(0).$$

In the limit of vanishing lepton mass, the form factors f_0 and A_0 do not contribute to the semileptonic decay rates. However, they contribute to nonleptonic decay rates in the factorization approximation.

It is convenient to consider B_c semileptonic and nonleptonic decays in the B_c meson rest frame. Then it is important to take into account the boost of the final meson wave function from the rest reference frame to the moving one with the recoil momentum $\mathbf{\Delta}$, given by Eq. (14). Now we can apply the method for calculating decay matrix elements described in the previous section. As it is argued above, the leading contributions arising from the vertex function $\Gamma^{(1)}$ can be exactly expressed through the overlap integrals of the meson wave functions in the whole kinematical range. For the subleading contribution $\Gamma^{(2)}$, the expansion in powers of the ratio of the relative quark momentum $\mathbf{p}$ to heavy quark masses $m_{b,c}$ should be performed taking into account that the recoil momentum of the final meson $\mathbf{\Delta}$ can be large. Such expansion is well justified for B_c decays to charmonium in the whole kinematical range. For B_c decays to D mesons, where one of the final quarks is light, a similar expansion is well justified only in the kinematical region of large recoil momentum. However, the numerical smallness of this subleading contribution due to its proportionality to the small meson binding energy permits its extrapolation to the whole kinematical range. As a result, we get the following expressions for the B_c decay form factors:

(a) $B_c \to P$ transitions ($P = \eta_c, D$)

$$f_+(q^2) = f_+^{(1)}(q^2) + \varepsilon f_+^{S(2)}(q^2) + (1-\varepsilon)f_+^{V(2)}(q^2), \tag{19}$$

$$f_0(q^2) = f_0^{(1)}(q^2) + \varepsilon f_0^{S(2)}(q^2) + (1-\varepsilon)f_0^{V(2)}(q^2), \tag{20}$$

(b) $B_c \to V$ transition ($V = \psi, D^*$)

$$V(q^2) = V^{(1)}(q^2) + \varepsilon V^{S(2)}(q^2) + (1-\varepsilon)V^{V(2)}(q^2), \tag{21}$$

$$A_1(q^2) = A_1^{(1)}(q^2) + \varepsilon A_1^{S(2)}(q^2) + (1-\varepsilon)A_1^{V(2)}(q^2), \tag{22}$$

$$A_2(q^2) = A_2^{(1)}(q^2) + \varepsilon A_2^{S(2)}(q^2) + (1-\varepsilon)A_2^{V(2)}(q^2), \tag{23}$$

TABLE I: Form factors of weak B_c decays ($b \to c, u$ transitions).

Transition	$f_+(q^2)$	$f_0(q^2)$	$V(q^2)$	$A_1(q^2)$	$A_2(q^2)$	$A_0(q^2)$
$B_c \to \eta_c, J/\psi$						
$q^2 = q^2_{\rm max}$	1.07	0.92	1.34	0.88	1.33	1.06
$q^2 = 0$	0.47	0.47	0.49	0.50	0.73	0.40
$B_c \to \eta_c', \psi'$						
$q^2 = q^2_{\rm max}$	0.08	0.05	−0.16	0.03	0.10	0.08
$q^2 = 0$	0.27	0.27	0.24	0.18	0.14	0.23
$B_c \to D, D^*$						
$q^2 = q^2_{\rm max}$	1.20	0.64	2.60	0.62	1.78	0.97
$q^2 = 0$	0.14	0.14	0.18	0.17	0.19	0.14

$$A_0(q^2) = A_0^{(1)}(q^2) + \varepsilon A_0^{S(2)}(q^2) + (1-\varepsilon) A_0^{V(2)}(q^2), \tag{24}$$

where $f_{+,0}^{(1)}$, $f_{+,0}^{S,V(2)}$, $A_{0,1,2}^{(1)}$, $A_{0,1,2}^{S,V(2)}$, $V^{(1)}$ and $V^{S,V(2)}$ are given in Appendix. The superscripts "(1)" and "(2)" correspond to Figs. 1 and 2, S and V to the scalar and vector potentials of $q\bar{q}$-interaction. The mixing parameter of scalar and vector confining potentials ε is fixed to be -1 in our model.

It is easy to check that in the heavy quark limit the decay matrix elements (16)–(18) with form factors (19)–(24) satisfy the heavy quark spin symmetry relations [15] obtained near the zero recoil point ($\mathbf{\Delta} \to 0$).

For numerical calculations we use the quasipotential wave functions of the B_c meson, charmonium and D mesons obtained in the mass spectra calculations [4, 5]. Our model predicts the B_c meson mass $M_{B_c} = 6.270$ GeV [9], while for J/ψ, η_c, ψ', η_c', D and D^* meson masses we use experimental data [16]. The calculated values of form factors at zero ($q^2 = q^2_{\rm max}$) and maximum ($q^2 = 0$) recoil of the final meson are listed in Table I. In Fig. 4 we plot leading $V^{(1)}$ and subleading $V^{S(2)}$, $V^{V(2)}$ contributions to the form factor V for $B_c \to D^*$ transition, as an example. We see that the leading contribution $V^{(1)}$ is dominant in the whole kinematical range, as it was expected. The subleading contributions $V^{S(2)}$, $V^{V(2)}$ are small and depend weakly on q^2. The behavior of corresponding contributions to other form factors is similar. This supports our conjecture that the formulae (A.1)–(A.18) can be applied for the calculation of the form factors of $B_c \to D^{(*)}$ transitions in the whole kinematical range.

In Figs. 5-10 we plot the calculated q^2 dependence of the weak form factors of Cabibbo-Kobayashi-Maskawa (CKM) favored $B_c \to \eta_c$, $B_c \to J/\psi$, $B_c \to \eta_c'$, $B_c \to \psi'$, as well as CKM suppressed $B_c \to D$, $B_c \to D^*$ transitions in the whole kinematical range. The different behavior (growing or falling with q^2) of the form factors displayed in Figs. 5-8 is evoked by the properties of the final meson wave functions, since the $2S$ wave function of the radially excited η', ψ' mesons has a zero.

In the following sections we use the obtained form factors for the calculation of the B_c semileptonic and nonleptonic decay rates.

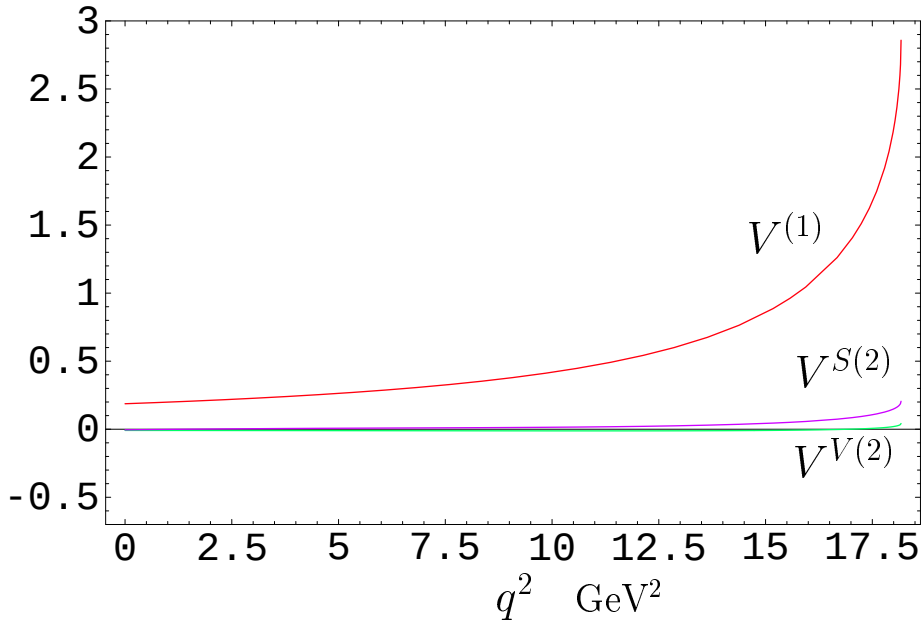

FIG. 4: Leading $V^{(1)}$ and subleading $V^{S(2)}$, $V^{V(2)}$ contributions to the form factor V for the $B_c \to D^*$ transition.

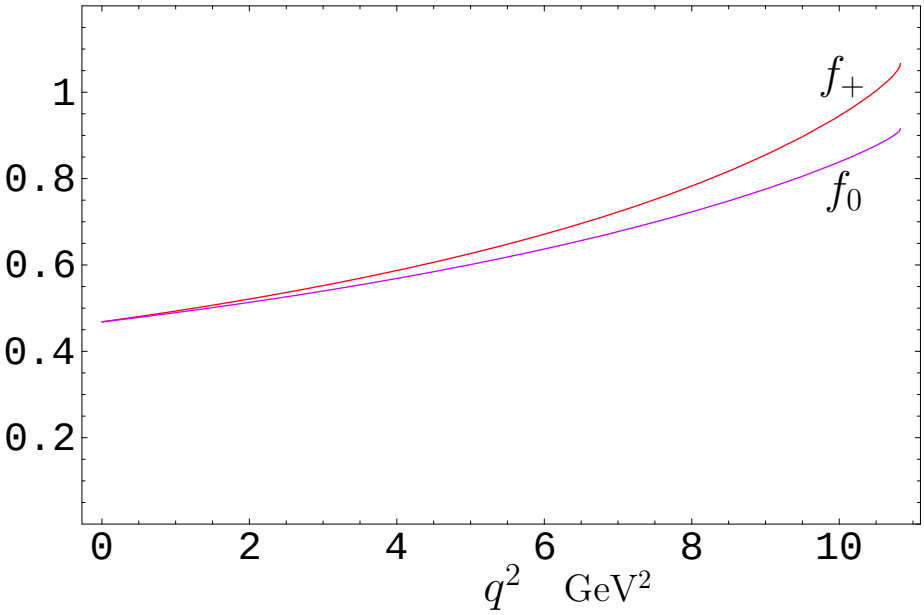

FIG. 5: Form factors of $B_c \to \eta_c e\nu$ decay.

V. SEMILEPTONIC DECAYS

The differential semileptonic decay rates can be expressed in terms of the form factors as follows.

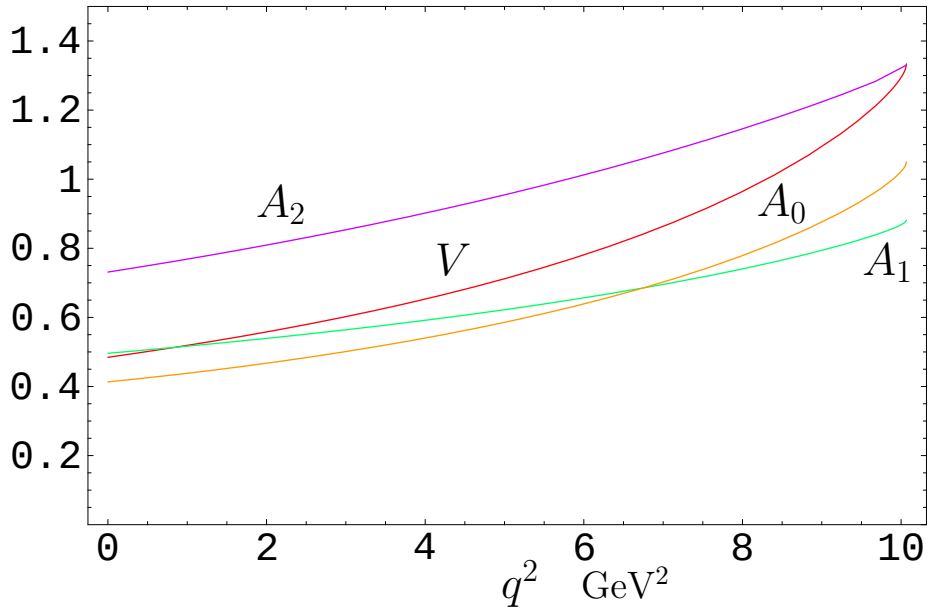

FIG. 6: Form factors of $B_c \to J/\psi e\nu$ decay.

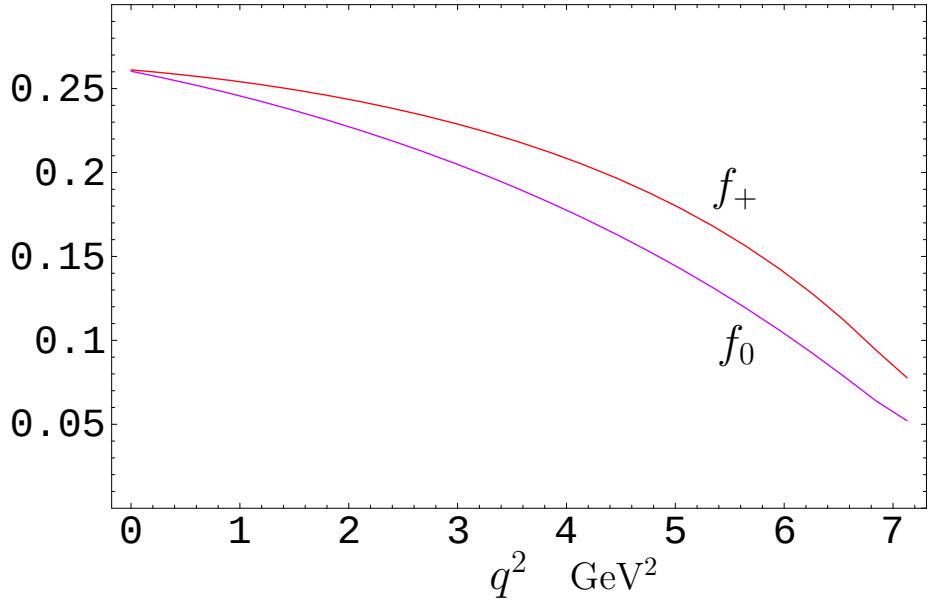

FIG. 7: Form factors of $B_c \to \eta_c' e\nu$ decay.

(a) $B_c \to Pe\nu$ decays ($P = \eta_c, D$)

$$\frac{\mathrm{d}\Gamma}{\mathrm{d}q^2}(B_c \to Pe\nu) = \frac{G_F^2 \Delta^3 |V_{qb}|^2}{24\pi^3} |f_+(q^2)|^2. \tag{25}$$

(b) $B_c \to Ve\nu$ decays ($V = \psi, D^*$)

$$\frac{\mathrm{d}\Gamma}{\mathrm{d}q^2}(B_c \to Ve\nu) = \frac{G_F^2 \Delta |V_{qb}|^2}{96\pi^3} \frac{q^2}{M_{B_c}^2} \left(|H_+(q^2)|^2 + |H_-(q^2)|^2 + |H_0(q^2)|^2 \right), \tag{26}$$

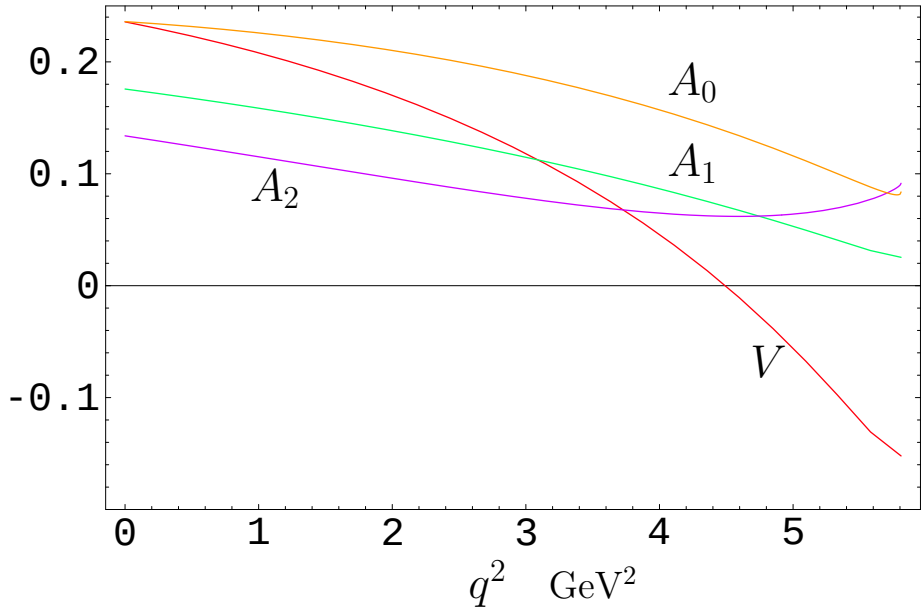

FIG. 8: Form factors of $B_c \to \psi' e\nu$ decay.

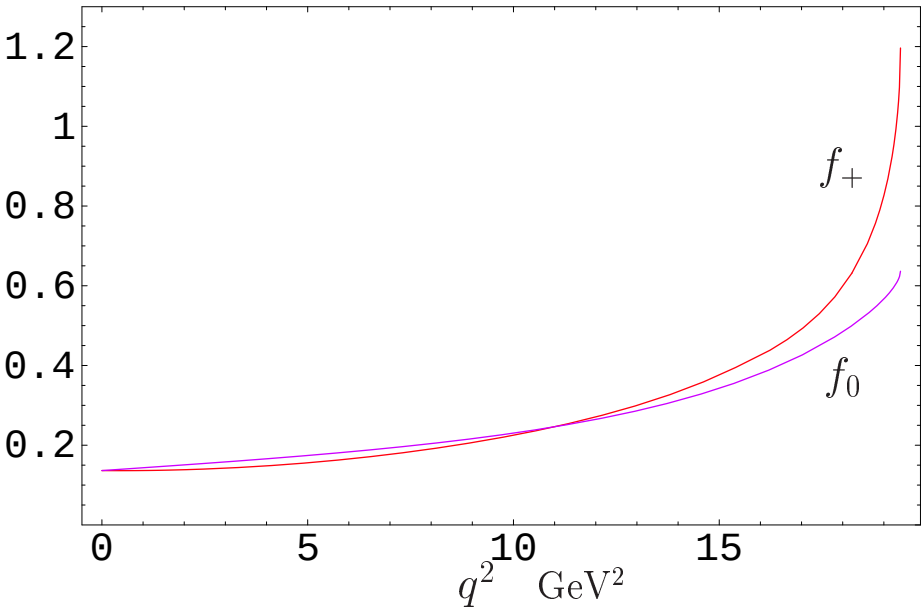

FIG. 9: Form factors of $B_c \to De\nu$ decay.

where G_F is the Fermi constant, V_{qb} is the CKM matrix element ($q = c, u$),

$$\Delta \equiv |\mathbf{\Delta}| = \sqrt{\frac{(M_{B_c}^2 + M_{P,V}^2 - q^2)^2}{4M_{B_c}^2} - M_{P,V}^2}.$$

The helicity amplitudes are given by

$$H_\pm(q^2) = \frac{2M_{B_c}\Delta}{M_{B_c} + M_V}\left[V(q^2) \mp \frac{(M_{B_c} + M_V)^2}{2M_{B_c}\Delta}A_1(q^2)\right], \tag{27}$$

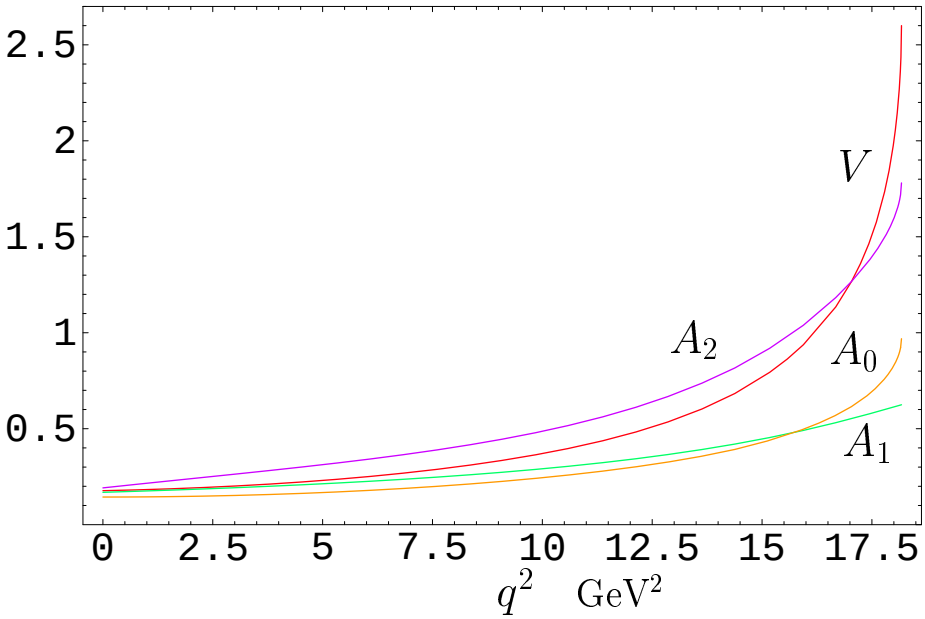

FIG. 10: Form factors of $B_c \to D^* e\nu$ decay.

$$H_0(q^2) = \frac{1}{2M_V\sqrt{q^2}}\left[(M_{B_c}+M_V)(M_{B_c}^2 - M_V^2 - q^2)A_1(q^2) - \frac{4M_{B_c}^2\Delta^2}{M_{B_c}+M_V}A_2(q^2)\right]. \quad (28)$$

The decay rates to the longitudinally and transversely polarized vector mesons are defined by

$$\frac{\mathrm{d}\Gamma_L}{\mathrm{d}q^2} = \frac{G_F^2\Delta|V_{qb}|^2}{96\pi^3}\frac{q^2}{M_{B_c}^2}|H_0(q^2)|^2, \quad (29)$$

$$\frac{\mathrm{d}\Gamma_T}{\mathrm{d}q^2} = \frac{\mathrm{d}\Gamma_+}{\mathrm{d}q^2} + \frac{\mathrm{d}\Gamma_-}{\mathrm{d}q^2} = \frac{G_F^2\Delta|V_{qb}|^2}{96\pi^3}\frac{q^2}{M_{B_c}^2}\left(|H_+(q^2)|^2 + |H_-(q^2)|^2\right). \quad (30)$$

In Figs. 11-16 we plot the differential semileptonic decay rates $\mathrm{d}\Gamma/\mathrm{d}q^2$ for semileptonic decays $B_c \to \eta_c(J/\psi)e\nu$, $B_c \to \eta_c'(\psi')e\nu$ and $B_c \to D(D^*)e\nu$ calculated in our model using Eqs. (25), (26) both with and without account of $1/m_{b,c}$ corrections to the decay form factors (A.1)–(A.18). [1] From these plots we see that relativistic effects related to heavy quarks increase semileptonic B_c decay rates to the pseudoscalar η_c, η_c' and D mesons, while semileptonic decay rates to vector J/ψ, ψ' and D^* mesons are decreased by them. The decay rates for $B_c \to \eta_c' e\nu$ and $B_c \to De\nu$ receive the largest $1/m_{b,c}$ corrections. This is not surprising since in the former decay the radially excited η_c' wave function has a zero, which considerably decreases the nonrelativistic contribution and thus increases the relative size of relativistic effects. In the latter decay, the role of relativistic effects is enhanced due to the relativistic light quark in the D meson.

We calculate the total rates of the semileptonic B_c decays to the ground and radially excited states of charmonium and D mesons integrating the corresponding differential decay rates over q^2. For calculations we use the following values of the CKM matrix elements: $|V_{cb}| = 0.041$, $|V_{ub}| = 0.0036$. The results are given in Table II in comparison with predictions

[1] Relativistic wave functions were used for both calculations.

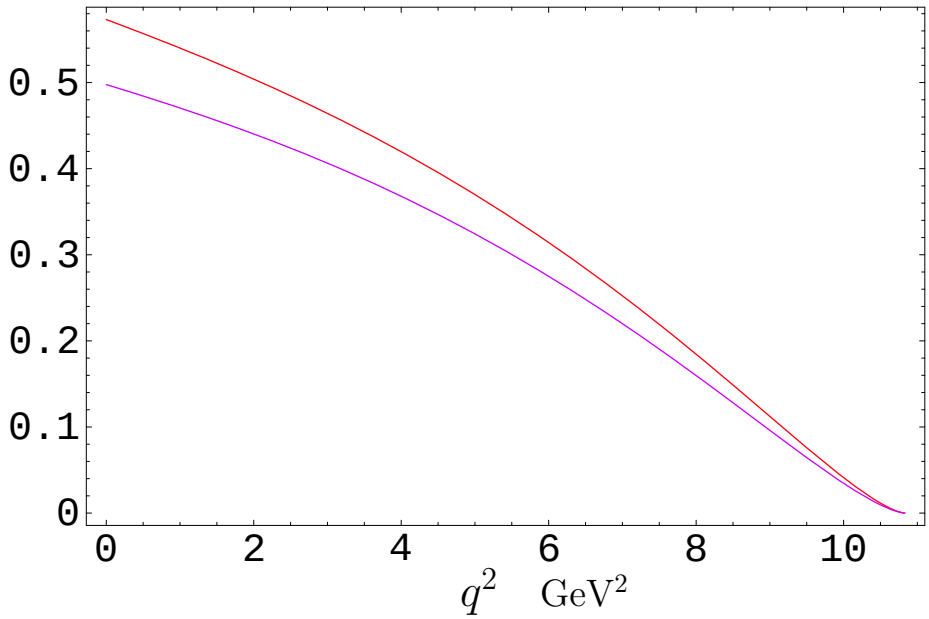

FIG. 11: Differential decay rates $(1/|V_{cb}|^2)\mathrm{d}\Gamma/\mathrm{d}q^2$ of $B_c \to \eta_c e\nu$ decay (in 10^{-12} GeV^{-1}). The lower curve is calculated without account of $1/m_{b,c}$ corrections.

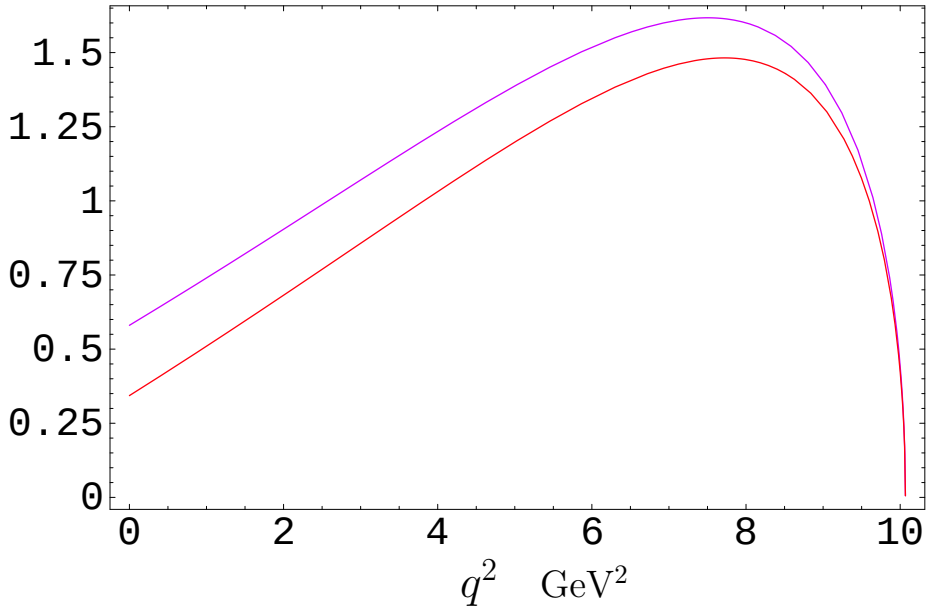

FIG. 12: Differential decay rates $(1/|V_{cb}|^2)\mathrm{d}\Gamma/\mathrm{d}q^2$ of $B_c \to J/\psi e\nu$ decay (in 10^{-12} GeV^{-1}). The upper curve is calculated without account of $1/m_{b,c}$ corrections.

of other approaches based on quark models [17, 19, 20, 22, 23, 25], QCD sum rules [18] and on the application of heavy quark symmetry relations [21, 24] to the quark model. Our predictions for the CKM favored semileptonic B_c decays to charmonium ground states are almost 2 times smaller than those of QCD sum rules [18] and quark models [17, 19, 20], but agree with quark model results [22–25]. Note that the ratios of the $B_c \to J/\psi e\nu$ to $B_c \to \eta_c e\nu$

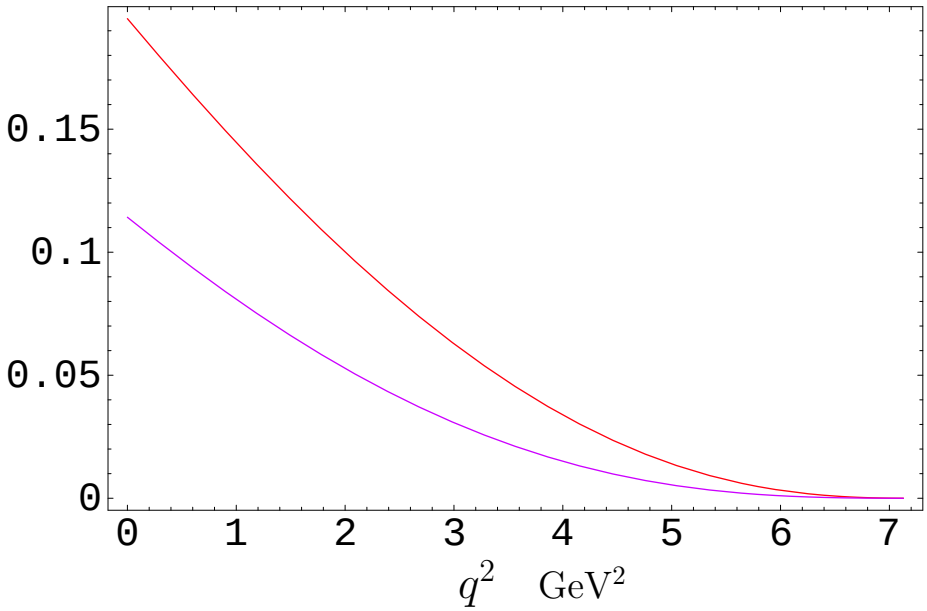

FIG. 13: Differential decay rates $(1/|V_{cb}|^2)\mathrm{d}\Gamma/\mathrm{d}q^2$ of $B_c \to \eta_c' e\nu$ decay (in 10^{-12} GeV^{-1}). The lower curve is calculated without account of $1/m_{b,c}$ corrections.

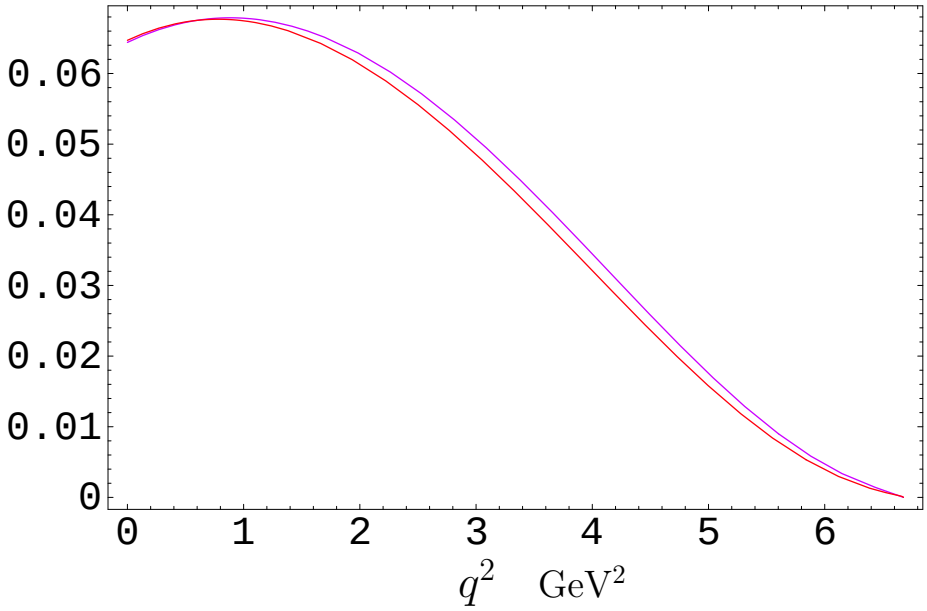

FIG. 14: Differential decay rates $(1/|V_{cb}|^2)\mathrm{d}\Gamma/\mathrm{d}q^2$ of $B_c \to \psi' e\nu$ decay (in 10^{-12} GeV^{-1}). The upper curve is calculated without account of $1/m_{b,c}$ corrections.

decay rates have close values in all approaches except [21]. In the case of semileptonic decays to radially excited charmonium states our prediction for the decay to the pseudoscalar η_c' state is consistent with others, while the one for the decay to ψ' is considerably smaller (with the exception of Ref. [25]). For the CKM suppressed semileptonic decays of B_c to D mesons our results are in agreement with those of Ref. [21].

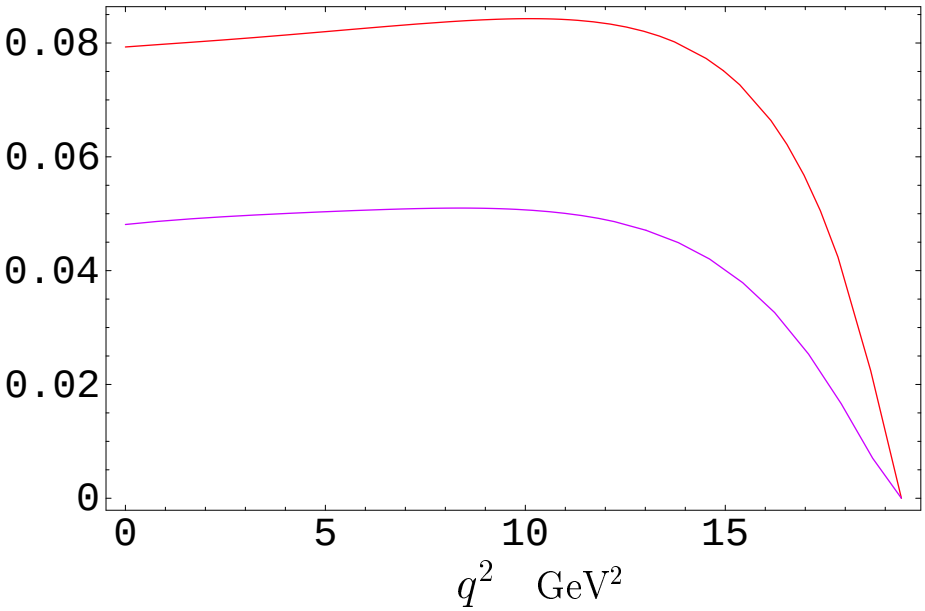

FIG. 15: Differential decay rate $(1/|V_{ub}|^2)\mathrm{d}\Gamma/\mathrm{d}q^2$ of $B_c \to De\nu$ decay (in 10^{-12} GeV^{-1}). The lower curve is calculated without account of $1/m_{b,c}$ corrections.

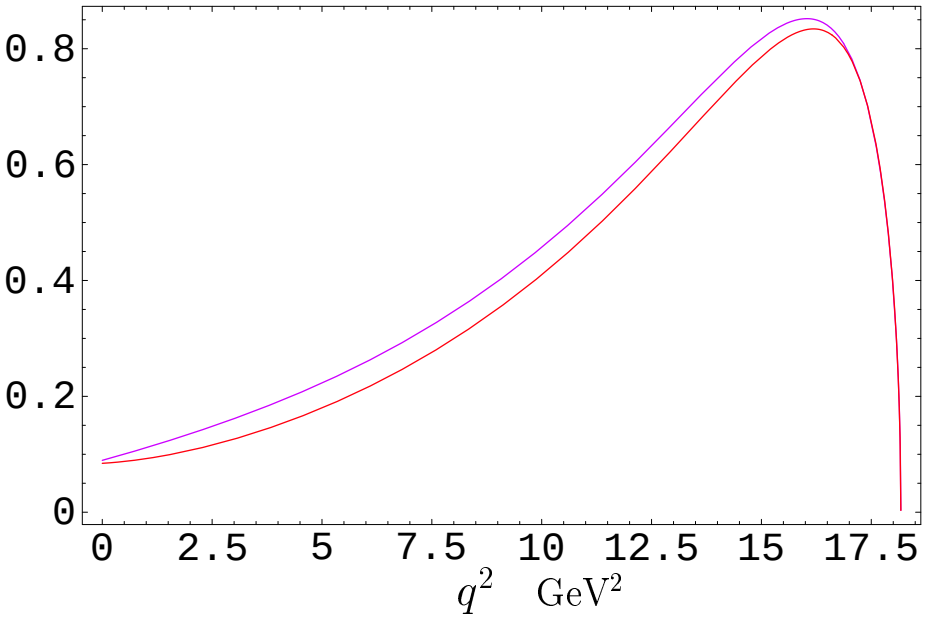

FIG. 16: Differential decay rates $(1/|V_{ub}|^2)\mathrm{d}\Gamma/\mathrm{d}q^2$ of $B_c \to D^* e\nu$ decay (in 10^{-12} GeV^{-1}). The upper curve is calculated without account of $1/m_{b,c}$ corrections.

In Table III we present for completeness our predictions for the rates of the semileptonic B_c decays to vector (ψ and D^*) mesons with longitudinal (L) or transverse (T) polarization and to the states with helicities $\lambda = \pm 1$, as well as their ratios.

TABLE II: Semileptonic decay rates Γ (in 10^{-15} GeV) of B_c decays to charmonium and D mesons.

Decay	our	[17]	[18]	[19]	[20]	[21]	[22]	[23]	[24]	[25]
$B_c \to \eta_c e\nu$	5.9	14	11	11.1	14.2	2.1(6.9)	8.6	6.8	4.3	8.31
$B_c \to \eta_c' e\nu$	0.46		0.60		0.73	0.3				0.605
$B_c \to J/\psi e\nu$	17.7	33	28	30.2	34.4	21.6(48.3)	17.5	19.4	16.8	20.3
$B_c \to \psi' e\nu$	0.44		1.94		1.45	1.7				0.186
$B_c \to D e\nu$	0.019	0.26	0.059	0.049	0.094	0.005(0.03)			0.001	0.0853
$B_c \to D^* e\nu$	0.11	0.49	0.27	0.192	0.269	0.12(0.5)			0.06	0.204

TABLE III: Semileptonic decay rates $\Gamma_{L,T,+,-}$ (in 10^{-15} GeV) and their ratios for B_c decays to vector ψ and D^* mesons.

Decay	Γ_L	Γ_T	Γ_L/Γ_T	Γ_+	Γ_-	Γ_+/Γ_-
$B_c \to J/\psi e\nu$	7.8	9.9	0.78	2.9	7.0	0.40
$B_c \to \psi' e\nu$	0.29	0.15	1.85	0.05	0.10	0.47
$B_c \to D^* e\nu$	0.04	0.07	0.53	0.015	0.055	0.24

VI. NONLEPTONIC DECAYS

In the standard model nonleptonic B_c decays are described by the effective Hamiltonian, obtained by integrating out the heavy W-boson and top quark. For the case of $b \to c, u$ transitions, one gets

$$H_{\rm eff} = \frac{G_F}{\sqrt{2}} V_{cb} \left[c_1(\mu) O_1^{cb} + c_2(\mu) O_2^{cb} \right] + \frac{G_F}{\sqrt{2}} V_{ub} \left[c_1(\mu) O_1^{ub} + c_2(\mu) O_2^{ub} \right] + \dots . \tag{31}$$

The Wilson coefficients $c_{1,2}(\mu)$ are evaluated perturbatively at the W scale and then are evolved down to the renormalization scale $\mu \approx m_b$ by the renormalization-group equations. The ellipsis denote the penguin operators, the Wilson coefficients of which are numerically much smaller than $c_{1,2}$. The local four-quark operators O_1 and O_2 are given by

$$\begin{aligned} O_1^{qb} &= [(\tilde{d}u)_{V-A} + (\tilde{s}c)_{V-A}](\bar{q}b)_{V-A}, \\ O_2^{qb} &= (\bar{q}u)_{V-A}(\tilde{d}b)_{V-A} + (\bar{q}c)_{V-A}(\tilde{s}b)_{V-A}, \qquad q = (u, c), \end{aligned} \tag{32}$$

where the rotated antiquark fields are

$$\tilde{d} = V_{ud}\bar{d} + V_{us}\bar{s}, \qquad \tilde{s} = V_{cd}\bar{d} + V_{cs}\bar{s}, \tag{33}$$

and for the hadronic current the following notation is used

$$(\bar{q}q')_{V-A} = \bar{q}\gamma_\mu(1-\gamma_5)q' \equiv J_\mu^W .$$

The factorization approach, which is extensively used for the calculation of two-body nonleptonic decays, such as $B_c \to FM$, assumes that the nonleptonic decay amplitude reduces to the product of a form factor and a decay constant [26]. This assumption in

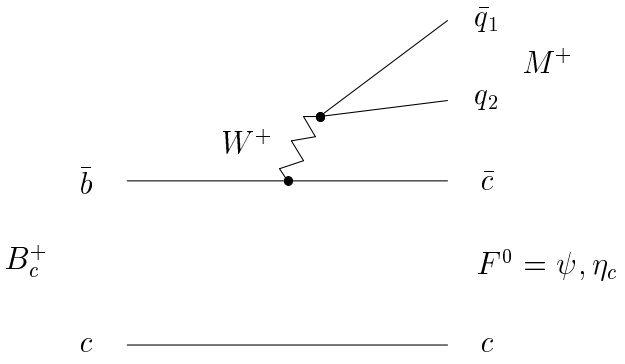

FIG. 17: Quark diagram for the nonleptonic $B_c^+ \to F^0 M^+$ decay.

general cannot be exact. However, it is expected that factorization can hold for the energetic decays, where the final F meson is heavy and the M meson is light [27]. A justification of this assumption is usually based on the issue of color transparency [28]. In these decays the final hadrons are produced in the form of point-like color-singlet objects with a large relative momentum. And thus the hadronization of the decay products occurs after they are too far away for strongly interacting with each other. That provides the possibility to avoid the final state interaction. A more general treatment of factorization is given in Refs. [29, 30].

In this paper we limit our analysis of the B_c^+ nonleptonic decays to the case when the final meson F^0 is charmonium [2] and the light M^+ meson is π^+, ρ^+ or $K^{(*)+}$. The corresponding diagram is shown in Fig. 17, where $q_1 = d$, s and $q_2 = u$. Then the decay amplitude can be approximated by the product of one-particle matrix elements

$$\langle F^0 M^+ | H_{\rm eff} | B_c^+ \rangle = \frac{G_F}{\sqrt{2}} V_{cb} V_{q_1 q_2} a_1 \langle F | (\bar{b}c)_{V-A} | B_c \rangle \langle M | (\bar{q}_1 q_2)_{V-A} | 0 \rangle, \tag{34}$$

where

$$a_1 = c_1(\mu) + \frac{1}{N_c} c_2(\mu) \tag{35}$$

and N_c is the number of colors.

The matrix element of the current J_μ^W between vacuum and final pseudoscalar (P) or vector (V) meson is parametrized by the decay constants $f_{P,V}$

$$\langle P | \bar{q}_1 \gamma^\mu \gamma_5 q_2 | 0 \rangle = i f_P p_P^\mu, \qquad \langle V | \bar{q}_1 \gamma_\mu q_2 | 0 \rangle = \epsilon_\mu M_V f_V. \tag{36}$$

We use the following values of the decay constants: $f_\pi = 0.131$ GeV, $f_\rho = 0.208$ GeV, $f_K = 0.160$ GeV and $f_{K^*} = 0.214$ GeV. The CKM matrix elements are $|V_{ud}| = 0.975$, $|V_{us}| = 0.222$.

The matrix elements of the weak current between the B_c meson and the final charmonium entering the factorized nonleptonic decay amplitude (34) are parametrized by the set of decay form factors defined in Eqs. (16) and (17). Using the form factor values calculated in Sec. IV, we get predictions for the nonleptonic $B_c^+ \to F^0 M^+$ decay rates and give them in Table IV in comparison with other calculations [18–22, 25]. We see that for most decays our model predicts slightly lower decay rates than other approaches.

[2] We do not consider nonleptonic B_c decays where the final meson F is a D meson, since such decays are strongly CKM suppressed and thus receive important contributions from the weak annihilation and penguins.

TABLE IV: Nonleptonic B_c decay rates Γ (in 10^{-15} GeV).

Decay	our	[18]	[19]	[20]	[22]	[21]	[25]
$B_c^+ \to \eta_c \pi^+$	$0.93a_1^2$	$1.8a_1^2$	$1.59a_1^2$	$2.07a_1^2$	$1.47a_1^2$	$0.28a_1^2$	$1.49a_1^2$
$B_c^+ \to \eta_c \rho^+$	$2.3a_1^2$	$4.5a_1^2$	$3.74a_1^2$	$5.48a_1^2$	$3.35a_1^2$	$0.75a_1^2$	$3.93a_1^2$
$B_c^+ \to J/\psi \pi^+$	$0.67a_1^2$	$1.43a_1^2$	$1.22a_1^2$	$1.97a_1^2$	$0.82a_1^2$	$1.48a_1^2$	$1.01a_1^2$
$B_c^+ \to J/\psi \rho^+$	$1.8a_1^2$	$4.37a_1^2$	$3.48a_1^2$	$5.95a_1^2$	$2.32a_1^2$	$4.14a_1^2$	$3.25a_1^2$
$B_c^+ \to \eta_c K^+$	$0.073a_1^2$	$0.15a_1^2$	$0.119a_1^2$	$0.161a_1^2$	$0.15a_1^2$	$0.023a_1^2$	$0.115a_1^2$
$B_c^+ \to \eta_c K^{*+}$	$0.12a_1^2$	$0.22a_1^2$	$0.200a_1^2$	$0.286a_1^2$	$0.24a_1^2$	$0.041a_1^2$	$0.198a_1^2$
$B_c^+ \to J/\psi K^+$	$0.052a_1^2$	$0.12a_1^2$	$0.090\ a_1^2$	$0.152a_1^2$	$0.079a_1^2$	$0.076a_1^2$	$0.0764a_1^2$
$B_c^+ \to J/\psi K^{*+}$	$0.11a_1^2$	$0.25a_1^2$	$0.197a_1^2$	$0.324a_1^2$	$0.18a_1^2$	$0.23a_1^2$	$0.174a_1^2$
$B_c^+ \to \eta_c' \pi^+$	$0.19a_1^2$			$0.268a_1^2$		$0.074a_1^2$	$0.248a_1^2$
$B_c^+ \to \eta_c' \rho^+$	$0.40a_1^2$			$0.622a_1^2$		$0.16a_1^2$	$0.587a_1^2$
$B_c^+ \to \psi' \pi^+$	$0.12a_1^2$			$0.252a_1^2$		$0.22a_1^2$	$0.0708a_1^2$
$B_c^+ \to \psi' \rho^+$	$0.20a_1^2$			$0.710\ a_1^2$		$0.54a_1^2$	$0.183a_1^2$
$B_c^+ \to \eta_c' K^+$	$0.014a_1^2$			$0.020a_1^2$		$0.0055a_1^2$	$0.0184a_1^2$
$B_c^+ \to \eta_c' K^{*+}$	$0.021a_1^2$			$0.031a_1^2$		$0.008a_1^2$	$0.0283a_1^2$
$B_c^+ \to \psi' K^+$	$0.009a_1^2$			$0.018a_1^2$		$0.01a_1^2$	$0.00499a_1^2$
$B_c^+ \to \psi' K^{*+}$	$0.011a_1^2$			$0.038\ a_1^2$		$0.03a_1^2$	$0.00909a_1^2$

VII. CONCLUSIONS

In this paper we calculated weak semileptonic and nonleptonic B_c decays to the charmonium and D meson final states. The corresponding decay form factors were calculated in the framework of the relativistic quark model using v/c expansion for the B_c meson and charmonium and heavy quark expansion for D mesons. These transitions proceed in a large kinematically allowed region. As a result, the recoil momentum $\mathbf{\Delta}$ of the final meson in the B_c rest frame is mostly large compared to the binding energy and the relative momentum of quarks forming a meson. Our approach permits to determine explicitly the dependence of form factors of the CKM favored B_c transition to charmonium in the whole kinematical region through the overlap integrals of the meson wave functions. This is a real achievement making our results more reliable, since most other approaches determine form factors only at the single point of zero ($q^2 = q^2_{\rm max}$) or maximum ($q^2 = 0$) recoil of the final meson and then the extrapolation is used. We calculated form factors of weak B_c transitions to charmonium up to second order corrections in the ratio of the relative quark momentum to the heavy (b and c) quark mass. In the case of the CKM suppressed B_c transitions to D mesons the situation is more complicated, since the active quark undergoes heavy-to-light transition. The leading contribution as in the previous case can be determined exactly, while the subleading contribution, which is suppressed by the small binding energy, can be determined reliably in most part of the kinematical range except a small region near the point of zero recoil ($q^2 = q^2_{\rm max}$) of the final D meson. As the numerical analysis shows, the extrapolation of form factors obtained in such a way to the region of small recoil introduces only minor uncertainties.

We calculated semileptonic and nonleptonic (in factorization approximation) B_c decay rates. Our predictions for the branching fractions are summarized in Table V, where we use

TABLE V: Branching fractions (in %) of exclusive B_c decays calculated for the fixed values of the B_c lifetime $\tau_{B_c} = 0.46$ ps and $a_1 = 1.14$.

Decay	Br	Decay	Br	Decay	Br
$B_c \to \eta_c e\nu$	0.42	$B_c^+ \to \eta_c \pi^+$	0.085	$B_c^+ \to \eta' \pi^+$	0.017
$B_c \to \eta_c' e\nu$	0.032	$B_c^+ \to \eta_c \rho^+$	0.21	$B_c^+ \to \eta_c' \rho^+$	0.036
$B_c \to J/\psi e\nu$	1.23	$B_c^+ \to J/\psi \pi^+$	0.061	$B_c^+ \to \psi' \pi^+$	0.011
$B_c \to \psi' e\nu$	0.031	$B_c^+ \to J/\psi \rho^+$	0.16	$B_c^+ \to \psi' \rho^+$	0.018
$B_c \to D e\nu$	0.013	$B_c^+ \to \eta_c K^+$	0.007	$B_c^+ \to \eta_c' K^+$	0.001
$B_c \to D^* e\nu$	0.037	$B_c^+ \to \eta_c K^{*+}$	0.011	$B_c^+ \to \eta_c' K^{*+}$	0.002
		$B_c^+ \to J/\psi K^+$	0.005	$B_c^+ \to \psi' K^+$	0.001
		$B_c^+ \to J/\psi K^{*+}$	0.010	$B_c^+ \to \psi' K^{*+}$	0.001

the central experimental value of the B_c meson lifetime [16]. From this table we see that the considered semileptonic decays to charmonium and D mesons give in total 1.72% of the B_c decay rate, while the energetic nonleptonic decays give additional 0.63%. It is expected that the dominant contribution to the B_c total rate comes from the charmed quark decays. These decays will be considered in a forthcoming publication.

Acknowledgments

The authors express their gratitude to M. Müller-Preussker and V. Savrin for support and discussions. Two of us (R.N.F and V.O.G.) were supported in part by the *Deutsche Forschungsgemeinschaft* under contract Eb 139/2-2.

APPENDIX: FORM FACTORS OF WEAK B_c DECAYS

(a) $B_c \to P$ transition ($P = \eta_c, D$)

$$
\begin{aligned}
f_+^{(1)}(q^2) \;=\; & \sqrt{\frac{E_P}{M_{B_c}}} \int \frac{\mathrm{d}^3 p}{(2\pi)^3} \bar{\Psi}_P \left(\mathbf{p} + \frac{2m_c}{E_P + M_P} \mathbf{\Delta} \right) \sqrt{\frac{\epsilon_q(p+\Delta) + m_q}{2\epsilon_q(p+\Delta)}} \sqrt{\frac{\epsilon_b(p) + m_b}{2\epsilon_b(p)}} \\
& \times \Bigg\{ 1 + \frac{M_{B_c} - E_P}{\epsilon_q(p+\Delta) + m_q} + \frac{(\mathbf{p}\mathbf{\Delta})}{\mathbf{\Delta}^2} \Bigg(\frac{\mathbf{\Delta}^2}{[\epsilon_q(p+\Delta) + m_q][\epsilon_b(p) + m_b]} + (M_{B_c} - E_P) \\
& \times \left(\frac{1}{\epsilon_q(p+\Delta) + m_q} + \frac{1}{\epsilon_b(p) + m_b} \right) \Bigg) + \frac{\mathbf{p}^2}{[\epsilon_q(p+\Delta) + m_q][\epsilon_b(p) + m_b]} \\
& + \frac{2}{3} \mathbf{p}^2 \Bigg(\frac{E_P - M_P}{[\epsilon_q(p+\Delta) + m_q][\epsilon_b(p) + m_b]} \left(\frac{1}{\epsilon_q(p+\Delta) + m_q} - \frac{1}{\epsilon_c(p) + m_c} \right) \\
& + \frac{M_{B_c} - E_P}{E_P + M_P} \left(\frac{1}{\epsilon_q(p+\Delta) + m_q} - \frac{1}{\epsilon_b(p) + m_b} \right) \\
& \times \left(\frac{1}{\epsilon_c(p) + m_c} - \frac{1}{\epsilon_q(p+\Delta) + m_q} \right) \Bigg) \Bigg\} \Psi_{B_c}(\mathbf{p}),
\end{aligned}
\tag{A.1}
$$

$$
\begin{aligned}
f_+^{S(2)}(q^2) \;=\; & \sqrt{\frac{E_P}{M_{B_c}}}\int\frac{\mathrm{d}^3p}{(2\pi)^3}\bar{\Psi}_P\left(\mathbf{p}+\frac{2m_c}{E_P+M_P}\mathbf{\Delta}\right)\sqrt{\frac{\epsilon_q(\Delta)+m_q}{2\epsilon_q(\Delta)}}\Bigg\{\frac{1}{\epsilon_q(\Delta)}\Bigg(\frac{\epsilon_q(\Delta)-m_q}{\epsilon_q(\Delta)+m_q}\\
& -\frac{M_{B_c}-E_P}{\epsilon_q(\Delta)+mq}\Bigg)\left[M_P-\epsilon_q\left(p+\frac{2m_c}{E_P+M_P}\Delta\right)-\epsilon_c\left(p+\frac{2m_c}{E_P+M_P}\Delta\right)\right]\\
& +\frac{(\mathbf{p\Delta})}{\mathbf{\Delta}^2}\Bigg(\Bigg[\frac{1}{2\epsilon_q(\Delta)}\left(\frac{\epsilon_q(\Delta)-m_q}{\epsilon_q(\Delta)+m_q}-\frac{M_{B_c}-E_P}{\epsilon_q(\Delta)+m_q}\right)-\frac{1}{2m_b}\Bigg(\frac{\epsilon_q(\Delta)-m_q}{\epsilon_b(\Delta)+m_b}\\
& +\frac{M_{B_c}-E_P}{\epsilon_b(\Delta)+m_b}\Bigg)\Bigg]\Bigg[M_{B_c}+M_P-\epsilon_b(p)-\epsilon_c(p)-\epsilon_q\left(p+\frac{2m_c}{E_P+M_P}\Delta\right)\\
& -\epsilon_c\left(p+\frac{2m_c}{E_P+M_P}\Delta\right)\Bigg]-\frac{\epsilon_q(\Delta)-m_q}{2m_b\epsilon_q(\Delta)}\left(1-\frac{M_{B_c}-E_P}{\epsilon_q(\Delta)+m_q}\right)\\
& \times\left[M_P-\epsilon_q\left(p+\frac{2m_c}{E_P+M_P}\Delta\right)-\epsilon_c\left(p+\frac{2m_c}{E_P+M_P}\Delta\right)\right]\Bigg)\Bigg\}\Psi_{B_c}(\mathbf{p}), \qquad \text{(A.2)}
\end{aligned}
$$

$$
\begin{aligned}
f_+^{V(2)}(q^2) \;=\; & \sqrt{\frac{E_P}{M_{B_c}}}\int\frac{\mathrm{d}^3p}{(2\pi)^3}\bar{\Psi}_P\left(\mathbf{p}+\frac{2m_c}{E_P+M_P}\mathbf{\Delta}\right)\sqrt{\frac{\epsilon_q(\Delta)+m_q}{2\epsilon_q(\Delta)}}\frac{(\mathbf{p\Delta})}{\mathbf{\Delta}^2}\frac{1}{2m_c}\\
& \times\Bigg\{\Bigg[(\epsilon_q(\Delta)-m_q)\left(\frac{1}{\epsilon_b(\Delta)+m_b}-\frac{1}{\epsilon_q(\Delta)+m_q}\right)+(M_{B_c}-E_P)\Bigg(\frac{1}{\epsilon_b(\Delta)+m_b}\\
& +\frac{1}{\epsilon_q(\Delta)+m_q}\Bigg)\Bigg]\Bigg[M_{B_c}+M_P-\epsilon_b(p)-\epsilon_c(p)-\epsilon_q\left(p+\frac{2m_c}{E_P+M_P}\Delta\right)\\
& -\epsilon_c\left(p+\frac{2m_c}{E_P+M_P}\Delta\right)\Bigg]+2\frac{\epsilon_q(\Delta)-m_q}{\epsilon_q(\Delta)}\left(\frac{\epsilon_q(\Delta)-m_q}{\epsilon_q(\Delta)+m_q}-\frac{M_{B_c}-E_P}{\epsilon_q(\Delta)+m_q}\right)\\
& \times[M_{B_c}-\epsilon_b(p)-\epsilon_c(p)]-\frac{2m_c(\epsilon_q(\Delta)-m_q)}{\epsilon_q(\Delta)[\epsilon_q(\Delta)+m_q]}\Bigg[M_P-\epsilon_q\left(p+\frac{2m_c}{E_P+M_P}\Delta\right)\\
& -\epsilon_c\left(p+\frac{2m_c}{E_P+M_P}\Delta\right)\Bigg]\Bigg\}\Psi_{B_c}(\mathbf{p}), \qquad \text{(A.3)}
\end{aligned}
$$

$$
\begin{aligned}
f_0^{(1)}(q^2) \;=\; & \frac{2\sqrt{E_PM_{B_c}}}{M_{B_c}^2-M_P^2}\int\frac{\mathrm{d}^3p}{(2\pi)^3}\bar{\Psi}_P\left(\mathbf{p}+\frac{2m_c}{E_P+M_P}\mathbf{\Delta}\right)\sqrt{\frac{\epsilon_q(p+\Delta)+m_q}{2\epsilon_q(p+\Delta)}}\sqrt{\frac{\epsilon_b(p)+m_b}{2\epsilon_b(p)}}\\
& \times\Bigg\{(E_P+M_P)\left(\frac{E_P-M_P}{\epsilon_q(p+\Delta)+m_q}+\frac{M_{B_c}-E_P}{E_P+M_P}\right)+(\mathbf{p\Delta})\Bigg(\frac{1}{\epsilon_q(p+\Delta)+m_q}\\
& +\frac{1}{\epsilon_b(p)+m_b}+\frac{M_{B_c}-E_P}{[\epsilon_q(p+\Delta)+m_q][\epsilon_b(p)+m_b]}\Bigg)+\frac{\mathbf{p}^2(M_{B_c}-E_P)}{[\epsilon_q(p+\Delta)+m_q][\epsilon_b(p)+m_b]}\\
& -\frac{2}{3}\mathbf{p}^2(E_P-M_P)\left(\frac{1}{\epsilon_q(p+\Delta)+m_q}-\frac{1}{\epsilon_c(p)+m_c}\right)\Bigg(\frac{1}{\epsilon_q(p+\Delta)+m_q}\\
& -\frac{1}{\epsilon_b(p)+m_b}-\frac{M_{B_c}-E_P}{[\epsilon_q(p+\Delta)+m_q][\epsilon_b(p)+m_b]}\Bigg)\Bigg\}\Psi_{B_c}(\mathbf{p}), \qquad \text{(A.4)}
\end{aligned}
$$

$$
f_0^{S(2)}(q^2) \;=\; \frac{2\sqrt{E_PM_{B_c}}}{M_{B_c}^2-M_P^2}\int\frac{\mathrm{d}^3p}{(2\pi)^3}\bar{\Psi}_P\left(\mathbf{p}+\frac{2m_c}{E_P+M_P}\mathbf{\Delta}\right)\sqrt{\frac{\epsilon_q(\Delta)+m_q}{2\epsilon_q(\Delta)}}(\epsilon_q(\Delta)-m_q)\Bigg\{\frac{1}{\epsilon_q(\Delta)}
$$

$$\times\left(\frac{M_{B_c}-E_P}{\epsilon_q(\Delta)+mq}-1\right)\left[M_P-\epsilon_q\left(p+\frac{2m_c}{E_P+M_P}\Delta\right)-\epsilon_c\left(p+\frac{2m_c}{E_P+M_P}\Delta\right)\right]$$
$$-\frac{(\mathbf{p}\boldsymbol{\Delta})}{\boldsymbol{\Delta}^2}\left(\left[\frac{\epsilon_q(\Delta)+m_q}{2m_b[\epsilon_b(\Delta)+m_b]}\left(1+\frac{M_{B_c}-E_P}{\epsilon_q(\Delta)+m_q}\right)-\frac{1}{2\epsilon_q(\Delta)}\left(\frac{M_{B_c}-E_P}{\epsilon_q(\Delta)+m_q}-1\right)\right]\right.$$
$$\times\left[M_{B_c}+M_P-\epsilon_b(p)-\epsilon_c(p)-\epsilon_q\left(p+\frac{2m_c}{E_P+M_P}\Delta\right)-\epsilon_c\left(p+\frac{2m_c}{E_P+M_P}\Delta\right)\right]$$
$$+\frac{\epsilon_q(\Delta)+m_q}{2m_b\epsilon_q(\Delta)}\left(\frac{M_{B_c}-E_P}{\epsilon_q(\Delta)+m_q}-\frac{\epsilon_q(\Delta)-m_q}{\epsilon_q(\Delta)+m_q}\right)\left[M_P-\epsilon_q\left(p+\frac{2m_c}{E_P+M_P}\Delta\right)\right.$$
$$\left.\left.-\epsilon_c\left(p+\frac{2m_c}{E_P+M_P}\Delta\right)\right]\right)\Bigg\}\Psi_{B_c}(\mathbf{p}), \tag{A.5}$$

$$f_0^{V(2)}(q^2) = \frac{2\sqrt{E_P M_{B_c}}}{M_{B_c}^2-M_P^2}\int\frac{\mathrm{d}^3p}{(2\pi)^3}\bar{\Psi}_P\left(\mathbf{p}+\frac{2m_c}{E_P+M_P}\boldsymbol{\Delta}\right)\sqrt{\frac{\epsilon_q(\Delta)+m_q}{2\epsilon_q(\Delta)}}\,\frac{(\mathbf{p}\boldsymbol{\Delta})}{2m_c}$$
$$\times\left\{\left[\frac{1}{\epsilon_b(\Delta)+m_b}\left(1+\frac{M_{B_c}-E_P}{\epsilon_q(\Delta)+m_q}\right)-\frac{m_c}{\epsilon_c(\Delta)[\epsilon_c(\Delta)+m_c]}\left(\frac{M_{B_c}-E_P}{\epsilon_q(\Delta)+m_q}-1\right)\right]\right.$$
$$\times\left[M_{B_c}+M_P-\epsilon_b(p)-\epsilon_c(p)-\epsilon_q\left(p+\frac{2m_c}{E_P+M_P}\Delta\right)-\epsilon_c\left(p+\frac{2m_c}{E_P+M_P}\Delta\right)\right]$$
$$+\frac{\epsilon_q(\Delta)-m_q}{\epsilon_q(\Delta)[\epsilon_q(\Delta)+m_q]}\left[M_{B_c}-\epsilon_b(p)-\epsilon_c(p)\right]-\frac{1}{\epsilon_q(\Delta)}\left(\frac{M_{B_c}-E_P}{\epsilon_q(\Delta)+m_q}-\frac{\epsilon_q(\Delta)-m_q}{\epsilon_q(\Delta)+m_q}\right)$$
$$\left.\times\left[M_P-\epsilon_q\left(p+\frac{2m_c}{E_P+M_P}\Delta\right)-\epsilon_c\left(p+\frac{2m_c}{E_P+M_P}\Delta\right)\right]\right\}\Psi_{B_c}(\mathbf{p}), \tag{A.6}$$

where

$$|\boldsymbol{\Delta}|=\sqrt{\frac{(M_{B_c}^2+M_P^2-q^2)^2}{4M_{B_c}^2}-M_P^2},$$

$$E_P=\sqrt{M_P^2+\boldsymbol{\Delta}^2},\quad \epsilon_Q(p+\lambda\Delta)=\sqrt{m_Q^2+(\mathbf{p}+\lambda\boldsymbol{\Delta})^2}\quad (Q=b,c,u),$$

and the subscript q corresponds to c or u quark for the final η_c or D meson, respectively.

(b) $B_c\to V$ transition ($V=\psi, D^*$)

$$V^{(1)}(q^2) = \frac{M_{B_c}+M_V}{2\sqrt{M_{B_c}M_V}}\int\frac{\mathrm{d}^3p}{(2\pi)^3}\bar{\Psi}_V\left(\mathbf{p}+\frac{2m_c}{E_V+M_V}\boldsymbol{\Delta}\right)\sqrt{\frac{\epsilon_q(p+\Delta)+m_q}{2\epsilon_q(p+\Delta)}}\sqrt{\frac{\epsilon_b(p)+m_b}{2\epsilon_b(p)}}$$
$$\times\frac{2\sqrt{E_V M_V}}{\epsilon_q(p+\Delta)+m_q}\left\{1+\frac{(\mathbf{p}\boldsymbol{\Delta})}{\boldsymbol{\Delta}^2}\left(1-\frac{\epsilon_q(p+\Delta)+m_q}{2m_b}\right)+\frac{2}{3}\frac{\mathbf{p}^2}{E_V+M_V}\right.$$
$$\left.\times\left(\frac{\epsilon_q(p+\Delta)+m_q}{2m_b[\epsilon_c(p)+m_c]}-\frac{1}{\epsilon_q(p+\Delta)+m_q}\right)\right\}\Psi_{B_c}(\mathbf{p}), \tag{A.7}$$

$$V^{S(2)}(q^2) = \frac{M_{B_c}+M_V}{2\sqrt{M_{B_c}M_V}}\int\frac{\mathrm{d}^3p}{(2\pi)^3}\bar{\Psi}_V\left(\mathbf{p}+\frac{2m_c}{E_V+M_V}\boldsymbol{\Delta}\right)\sqrt{\frac{\epsilon_q(\Delta)+m_q}{2\epsilon_q(\Delta)}}\frac{2\sqrt{E_V M_V}}{\epsilon_q(\Delta)+m_q}$$

$$\times\Bigg\{-\frac{1}{\epsilon_q(\Delta)}\left[M_V-\epsilon_q\left(p+\frac{2m_c}{E_V+M_V}\Delta\right)-\epsilon_c\left(p+\frac{2m_c}{E_V+M_V}\Delta\right)\right]$$
$$-\frac{(\mathbf{p}\boldsymbol{\Delta})}{\boldsymbol{\Delta}^2}\frac{1}{2}\Bigg(\left(\frac{1}{\epsilon_q(\Delta)}-\frac{\epsilon_q(\Delta)+m_q}{m_b[\epsilon_b(\Delta)+m_b]}\right)\Bigg[M_{B_c}+M_V-\epsilon_b(p)-\epsilon_c(p)$$
$$-\epsilon_q\left(p+\frac{2m_c}{E_V+M_V}\Delta\right)-\epsilon_c\left(p+\frac{2m_c}{E_V+M_V}\Delta\right)\Bigg]+\frac{\epsilon_q(\Delta)-m_q}{2m_b\epsilon_q(\Delta)}$$
$$\times\left[M_V-\epsilon_q\left(p+\frac{2m_c}{E_V+M_V}\Delta\right)-\epsilon_c\left(p+\frac{2m_c}{E_V+M_V}\Delta\right)\right]\Bigg)\Bigg\}\Psi_{B_c}(\mathbf{p}), \quad \text{(A.8)}$$

$$V^{V(2)}(q^2) = \frac{M_{B_c}+M_V}{2\sqrt{M_{B_c}M_V}}\int\frac{\mathrm{d}^3p}{(2\pi)^3}\bar{\Psi}_V\left(\mathbf{p}+\frac{2m_c}{E_V+M_V}\boldsymbol{\Delta}\right)\sqrt{\frac{\epsilon_q(\Delta)+m_q}{2\epsilon_q(\Delta)}}\frac{2\sqrt{E_VM_V}}{\epsilon_q(\Delta)+m_q}$$
$$\times\frac{(\mathbf{p}\boldsymbol{\Delta})}{\boldsymbol{\Delta}^2}\frac{1}{2m_c}\left(\frac{m_q}{\epsilon_q(\Delta)}-\frac{\epsilon_q(\Delta)+m_q}{\epsilon_b(\Delta)+m_b}\right)\Bigg[M_{B_c}+M_V-\epsilon_b(p)-\epsilon_c(p)$$
$$-\epsilon_q\left(p+\frac{2m_c}{E_V+M_V}\Delta\right)-\epsilon_c\left(p+\frac{2m_c}{E_V+M_V}\Delta\right)\Bigg]\Psi_{B_c}(\mathbf{p}), \quad \text{(A.9)}$$

$$A_1^{(1)}(q^2) = \frac{2\sqrt{M_{B_c}M_V}}{M_{B_c}+M_V}\sqrt{\frac{E_V}{M_V}}\int\frac{\mathrm{d}^3p}{(2\pi)^3}\bar{\Psi}_V\left(\mathbf{p}+\frac{2m_c}{E_V+M_V}\boldsymbol{\Delta}\right)\sqrt{\frac{\epsilon_q(p+\Delta)+m_q}{2\epsilon_q(p+\Delta)}}\sqrt{\frac{\epsilon_b(p)+m_b}{2\epsilon_b(p)}}$$
$$\times\left\{1+\frac{1}{2m_b[\epsilon_q(p+\Delta)+m_q]}\left[\frac{2}{3}\mathbf{p}^2\frac{E_V-M_V}{\epsilon_c(p)+m_c}-\frac{\mathbf{p}^2}{3}-(\mathbf{p}\boldsymbol{\Delta})\right]\right\}\Psi_{B_c}(\mathbf{p}), \quad \text{(A.10)}$$

$$A_1^{S(2)}(q^2) = \frac{2\sqrt{M_{B_c}M_V}}{M_{B_c}+M_V}\sqrt{\frac{E_V}{M_V}}\int\frac{\mathrm{d}^3p}{(2\pi)^3}\bar{\Psi}_V\left(\mathbf{p}+\frac{2m_c}{E_V+M_V}\boldsymbol{\Delta}\right)\sqrt{\frac{\epsilon_q(\Delta)+m_q}{2\epsilon_q(\Delta)}}$$
$$\times\Bigg\{\frac{\epsilon_q(\Delta)-m_q}{\epsilon_q(\Delta)[\epsilon_q(\Delta)+m_q]}\left[M_V-\epsilon_q\left(p+\frac{2m_c}{E_V+M_V}\Delta\right)-\epsilon_c\left(p+\frac{2m_c}{E_V+M_V}\Delta\right)\right]$$
$$+\frac{(\mathbf{p}\boldsymbol{\Delta})}{\boldsymbol{\Delta}^2}\frac{\epsilon_q(\Delta)-m_q}{2}\Bigg(\left(\frac{1}{\epsilon_q(\Delta)[\epsilon_q(\Delta)+m_q]}+\frac{1}{m_b[\epsilon_b(\Delta)+m_b]}\right)\Bigg[M_{B_c}+M_V$$
$$-\epsilon_b(p)-\epsilon_c(p)-\epsilon_q\left(p+\frac{2m_c}{E_V+M_V}\Delta\right)-\epsilon_c\left(p+\frac{2m_c}{E_V+M_V}\Delta\right)\Bigg]+\frac{1}{m_b\epsilon_q(\Delta)}$$
$$\times\left[M_V-\epsilon_q\left(p+\frac{2m_c}{E_V+M_V}\Delta\right)-\epsilon_c\left(p+\frac{2m_c}{E_V+M_V}\Delta\right)\right]\Bigg)\Bigg\}\Psi_{B_c}(\mathbf{p}), \quad \text{(A.11)}$$

$$A_1^{V(2)}(q^2) = \frac{2\sqrt{M_{B_c}M_V}}{M_{B_c}+M_V}\sqrt{\frac{E_V}{M_V}}\int\frac{\mathrm{d}^3p}{(2\pi)^3}\bar{\Psi}_V\left(\mathbf{p}+\frac{2m_c}{E_V+M_V}\boldsymbol{\Delta}\right)\sqrt{\frac{\epsilon_q(\Delta)+m_q}{2\epsilon_q(\Delta)}}$$
$$\times\frac{(\mathbf{p}\boldsymbol{\Delta})}{\boldsymbol{\Delta}^2}\frac{\epsilon_q(\Delta)-m_q}{2m_c}\Bigg\{\frac{1}{\epsilon_q(\Delta)}\Bigg(\frac{\epsilon_q(\Delta)-m_q}{\epsilon_q(\Delta)+m_q}[M_{B_c}-\epsilon_b(p)-\epsilon_c(p)]$$
$$-\left[M_V-\epsilon_q\left(p+\frac{2m_c}{E_V+M_V}\Delta\right)-\epsilon_c\left(p+\frac{2m_c}{E_V+M_V}\Delta\right)\right]\Bigg)$$
$$-\left(\frac{1}{\epsilon_b(\Delta)+m_b}+\frac{m_q}{\epsilon_q(\Delta)[\epsilon_q(\Delta)+m_q]}\right)\Bigg[M_{B_c}+M_V-\epsilon_b(p)-\epsilon_c(p)$$

$$-\epsilon_q\left(p+\frac{2m_c}{E_V+M_V}\Delta\right)-\epsilon_c\left(p+\frac{2m_c}{E_V+M_V}\Delta\right)\Bigg]\Bigg\}\Psi_{B_c}(\mathbf{p}), \tag{A.12}$$

$$\begin{aligned}
A_2^{(1)}(q^2) \;=\; & \frac{M_{B_c}+M_V}{2\sqrt{M_{B_c}M_V}}\frac{2\sqrt{E_VM_V}}{E_V+M_V}\int\frac{\mathrm{d}^3p}{(2\pi)^3}\bar{\Psi}_V\left(\mathbf{p}+\frac{2m_c}{E_V+M_V}\mathbf{\Delta}\right)\sqrt{\frac{\epsilon_q(p+\Delta)+m_q}{2\epsilon_q(p+\Delta)}}\\
&\times\sqrt{\frac{\epsilon_b(p)+m_b}{2\epsilon_b(p)}}\Bigg\{1+\frac{M_V}{M_{B_c}}\left(1-\frac{E_V+M_V}{\epsilon_q(p+\Delta)+m_q}\right)-\frac{(\mathbf{p\Delta})}{\mathbf{\Delta}^2}\frac{E_V+M_V}{\epsilon_q(p+\Delta)+m_q}\\
&\times\Bigg(\frac{E_V+M_V}{2m_b}\left[1-\frac{M_V}{M_{B_c}}\left(1-\frac{\epsilon_q(p+\Delta)+m_q}{E_V+M_V}\right)\right]+\frac{M_V}{M_{B_c}}\Bigg)\\
&+\frac{2}{3}\frac{\mathbf{p}^2}{\epsilon_q(p+\Delta)+m_q}\Bigg(\frac{1}{2m_b}\Bigg[\frac{E_V+M_V}{\epsilon_c(p)+m_c}-\frac{1}{2}+\frac{M_V}{\epsilon_q(p+\Delta)+m_q}\\
&+\frac{M_V}{M_{B_c}}\left(\frac{\epsilon_q(p+\Delta)+m_q}{\epsilon_c(p)+m_c}-\frac{E_V+M_V}{\epsilon_c(p)+m_c}+\frac{1}{2}-\frac{E_V}{\epsilon_q(p+\Delta)+m_q}\right)\Bigg]\\
&+\frac{M_V}{M_{B_c}}\left(\frac{1}{\epsilon_q(p+\Delta)+m_q}+\frac{1}{\epsilon_c(p)+m_c}\right)\Bigg)\Bigg\}\Psi_{B_c}(\mathbf{p}),
\end{aligned} \tag{A.13}$$

$$\begin{aligned}
A_2^{S(2)}(q^2) \;=\; & \frac{M_{B_c}+M_V}{2\sqrt{M_{B_c}M_V}}\frac{2\sqrt{E_VM_V}}{E_V+M_V}\int\frac{\mathrm{d}^3p}{(2\pi)^3}\bar{\Psi}_V\left(\mathbf{p}+\frac{2m_c}{E_V+M_V}\mathbf{\Delta}\right)\sqrt{\frac{\epsilon_q(\Delta)+m_q}{2\epsilon_q(\Delta)}}\\
&\times\Bigg\{\frac{1}{\epsilon_q(\Delta)}\left[\frac{\epsilon_q(\Delta)-m_q}{\epsilon_q(\Delta)+m_q}+\frac{M_V}{M_{B_c}}\left(\frac{E_V+M_V}{\epsilon_q(\Delta)+m_q}+\frac{\epsilon_q(\Delta)-m_q}{\epsilon_q(\Delta)+m_q}\right)\right]\\
&\times\left[M_V-\epsilon_q\left(p+\frac{2m_c}{E_V+M_V}\Delta\right)-\epsilon_c\left(p+\frac{2m_c}{E_V+M_V}\Delta\right)\right]\\
&+\frac{(\mathbf{p\Delta})}{\mathbf{\Delta}^2}\Bigg(\Bigg(\frac{1}{2\epsilon_q(\Delta)}\left[\frac{\epsilon_q(\Delta)-m_q}{\epsilon_q(\Delta)+m_q}+\frac{M_V}{M_{B_c}}\left(\frac{E_V+M_V}{\epsilon_q(\Delta)+m_q}+\frac{\epsilon_q(\Delta)-m_q}{\epsilon_q(\Delta)+m_q}\right)\right]\\
&+\frac{1}{2m_b}\Bigg(\frac{\epsilon_q(\Delta)-m_q}{\epsilon_b(\Delta)+m_b}+2\frac{M_V(E_V+M_V)}{[\epsilon_q(\Delta)+m_q][\epsilon_b(\Delta)+m_b]}+\frac{M_V}{M_{B_c}}\Bigg[\frac{\epsilon_q(\Delta)-m_q}{\epsilon_b(\Delta)+m_b}\\
&+\frac{E_V+M_V}{\epsilon_b(\Delta)+m_b}\left(1-\frac{2E_V}{\epsilon_q(\Delta)+m_q}\right)\Bigg]\Bigg)\Bigg)\Bigg[M_{B_c}+M_V-\epsilon_b(p)-\epsilon_c(p)\\
&-\epsilon_q\left(p+\frac{2m_c}{E_V+M_V}\Delta\right)-\epsilon_c\left(p+\frac{2m_c}{E_V+M_V}\Delta\right)\Bigg]+\frac{1}{2m_b}\Bigg(\frac{\epsilon_q(\Delta)-m_q}{\epsilon_q(\Delta)}\\
&+2\frac{M_V(E_V+M_V)}{\epsilon_q(\Delta)[\epsilon_q(\Delta)+m_q]}+\frac{M_V}{M_{B_c}}\Bigg[\frac{\epsilon_q(\Delta)-m_q}{\epsilon_q(\Delta)}\left(1-\frac{E_V+M_V}{\epsilon_q(\Delta)+m_q}\right)\\
&-2\frac{E_V(E_V+M_V)}{\epsilon_q(\Delta)[\epsilon_q(\Delta)+m_q]}\Bigg]\Bigg)\Bigg[M_V-\epsilon_q\left(p+\frac{2m_c}{E_V+M_V}\Delta\right)\\
&-\epsilon_c\left(p+\frac{2m_c}{E_V+M_V}\Delta\right)\Bigg]\Bigg)\Bigg\}\Psi_{B_c}(\mathbf{p}),
\end{aligned} \tag{A.14}$$

$$\begin{aligned}
A_2^{V(2)}(q^2) \;=\; & \frac{M_{B_c}+M_V}{2\sqrt{M_{B_c}M_V}}\frac{2\sqrt{E_VM_V}}{E_V+M_V}\int\frac{\mathrm{d}^3p}{(2\pi)^3}\bar{\Psi}_V\left(\mathbf{p}+\frac{2m_c}{E_V+M_V}\mathbf{\Delta}\right)\sqrt{\frac{\epsilon_q(\Delta)+m_q}{2\epsilon_q(\Delta)}}\\
&\times\frac{(\mathbf{p\Delta})}{\mathbf{\Delta}^2}\frac{1}{2m_c}\Bigg\{\frac{\epsilon_q(\Delta)-m_q}{\epsilon_q(\Delta)}\Bigg(-\frac{m_q}{\epsilon_q(\Delta)+m_q}\left(1+\frac{M_V}{M_{B_c}}\right)[M_{B_c}-\epsilon_b(p)-\epsilon_c(p)]
\end{aligned}$$

$$
\begin{aligned}
&+\left[1+\frac{M_V}{M_{B_c}}\left(1+\frac{E_V+M_V}{\epsilon_q(\Delta)+m_q}\right)\right]\Big[M_{B_c}-M_V-\epsilon_b(p)-\epsilon_c(p)\\
&+\epsilon_q\left(p+\frac{2m_c}{E_V+M_V}\Delta\right)+\epsilon_c\left(p+\frac{2m_c}{E_V+M_V}\Delta\right)\Big]\Big)\\
&+\Bigg(2\frac{M_V(E_V+M_V)}{[\epsilon_q(\Delta)+m_q][\epsilon_b(\Delta)+m_b]}\left(\frac{E_V}{M_V}-1\right)-\left(\frac{\epsilon_q(\Delta)+m_q}{\epsilon_b(\Delta)+m_b}+\frac{m_q}{\epsilon_q(\Delta)}\right)\\
&\times\left[\frac{\epsilon_q(\Delta)-m_q}{\epsilon_q(\Delta)+m_q}+\frac{M_V}{M_{B_c}}\left(\frac{\epsilon_q(\Delta)-m_q}{\epsilon_q(\Delta)+m_q}+\frac{E_V+M_V}{\epsilon_q(\Delta)+m_q}\right)\right]\Bigg)\Big[M_{B_c}+M_V-\epsilon_b(p)\\
&-\epsilon_c(p)-\epsilon_q\left(p+\frac{2m_c}{E_V+M_V}\Delta\right)-\epsilon_c\left(p+\frac{2m_c}{E_V+M_V}\Delta\right)\Big]\Bigg\}\Psi_{B_c}(\mathbf{p}), \qquad \text{(A.15)}
\end{aligned}
$$

$$
\begin{aligned}
A_0^{(1)}(q^2) \;=\; &\sqrt{\frac{E_V}{M_V}}\int\frac{\mathrm{d}^3p}{(2\pi)^3}\bar{\Psi}_V\left(\mathbf{p}+\frac{2m_c}{E_V+M_V}\boldsymbol{\Delta}\right)\sqrt{\frac{\epsilon_q(p+\Delta)+m_q}{2\epsilon_q(p+\Delta)}}\sqrt{\frac{\epsilon_b(p)+m_b}{2\epsilon_b(p)}}\\
&\times\Bigg\{1+\frac{M_{B_c}-E_V}{\epsilon_q(p+\Delta)+m_q}\Bigg(1+\left[\frac{(\mathbf{p}\boldsymbol{\Delta})}{\boldsymbol{\Delta}^2}-\frac{2}{3}\frac{\mathbf{p}^2}{E_V+M_V}\left(\frac{1}{\epsilon_q(p+\Delta)+m_q}\right.\right.\\
&\left.\left.+\frac{1}{\epsilon_c(p)+m_c}\right)\right]\left[1+\frac{1}{2m_b}\left(\frac{\boldsymbol{\Delta}^2}{M_{B_c}-E_V}+\epsilon_q(p+\Delta)+m_q\right)\right]\Bigg)\\
&-\frac{\mathbf{p}^2}{6m_b[\epsilon_q(p+\Delta)+m_q]}\Bigg\}\Psi_{B_c}(\mathbf{p}), \qquad \text{(A.16)}
\end{aligned}
$$

$$
\begin{aligned}
A_0^{S(2)}(q^2) \;=\; &\sqrt{\frac{E_V}{M_V}}\int\frac{\mathrm{d}^3p}{(2\pi)^3}\bar{\Psi}_V\left(\mathbf{p}+\frac{2m_c}{E_V+M_V}\boldsymbol{\Delta}\right)\sqrt{\frac{\epsilon_q(\Delta)+m_q}{2\epsilon_q(\Delta)}}\Bigg\{-\frac{M_{B_c}-E_V}{\epsilon_q(\Delta)+m_q}\frac{1}{\epsilon_q(\Delta)}\\
&\times\left(1-\frac{\epsilon_q(\Delta)-m_q}{M_{B_c}-E_V}\right)\left[M_V-\epsilon_q\left(p+\frac{2m_c}{E_V+M_V}\Delta\right)-\epsilon_c\left(p+\frac{2m_c}{E_V+M_V}\Delta\right)\right]\\
&+\frac{(\mathbf{p}\boldsymbol{\Delta})}{\boldsymbol{\Delta}^2}\Bigg((M_{B_c}-E_V)\left[\frac{1}{2\epsilon_q(\Delta)[\epsilon_q(\Delta)+m_q]}\left(1+\frac{\epsilon_q(\Delta)-m_q}{M_{B_c}-E_V}\right)\right.\\
&\left.+\frac{1}{2m_b[\epsilon_b(\Delta)+m_b]}\left(1-\frac{\epsilon_q(\Delta)-m_q}{M_{B_c}-E_V}\right)\right]\Big[M_{B_c}+M_V-\epsilon_b(p)-\epsilon_c(p)\\
&-\epsilon_q\left(p+\frac{2m_c}{E_V+M_V}\Delta\right)-\epsilon_c\left(p+\frac{2m_c}{E_V+M_V}\Delta\right)\Big]-\frac{1}{2m_b}\frac{\epsilon_q(\Delta)-m_q}{\epsilon_q(\Delta)}\\
&\times\left(1+\frac{M_{B_c}-E_V}{\epsilon_q(\Delta)+m_q}\right)\Big[M_V-\epsilon_q\left(p+\frac{2m_c}{E_V+M_V}\Delta\right)\\
&-\epsilon_c\left(p+\frac{2m_c}{E_V+M_V}\Delta\right)\Big]\Bigg)\Bigg\}\Psi_{B_c}(\mathbf{p}), \qquad \text{(A.17)}
\end{aligned}
$$

$$
\begin{aligned}
A_0^{V(2)}(q^2) \;=\; &\sqrt{\frac{E_V}{M_V}}\int\frac{\mathrm{d}^3p}{(2\pi)^3}\bar{\Psi}_V\left(\mathbf{p}+\frac{2m_c}{E_V+M_V}\boldsymbol{\Delta}\right)\sqrt{\frac{\epsilon_q(\Delta)+m_q}{2\epsilon_q(\Delta)}}\frac{(\mathbf{p}\boldsymbol{\Delta})}{\boldsymbol{\Delta}^2}\frac{1}{2m_c}\\
&\times\Bigg\{(M_{B_c}-E_V)\left[\frac{1}{\epsilon_b(\Delta)+m_b}\left(1+\frac{\epsilon_q(\Delta)-m_q}{M_{B_c}-E_V}\right)+\frac{m_q}{\epsilon_q(\Delta)[\epsilon_q(\Delta)+m_q]}\right.\\
&\left.\times\left(1-\frac{\epsilon_q(\Delta)-m_q}{M_{B_c}-E_V}\right)\right]\left[M_{B_c}+M_V-\epsilon_b(p)-\epsilon_c(p)-\epsilon_q\left(p+\frac{2m_c}{E_V+M_V}\Delta\right)\right.
\end{aligned}
$$

$$-\epsilon_c\left(p+\frac{2m_c}{E_V+M_V}\Delta\right)\Bigg] - \frac{\epsilon_q(\Delta)-m_q}{\epsilon_q(\Delta)}\Bigg(M_{B_c}-\epsilon_b(p)-\epsilon_c(p)$$
$$-\left(1-\frac{M_{B_c}-E_V}{\epsilon_q(\Delta)+m_q}\right)\left[M_{B_c}-M_V-\epsilon_b(p)-\epsilon_c(p)+\epsilon_q\left(p+\frac{2m_c}{E_V+M_V}\Delta\right)\right.$$
$$\left.+\epsilon_c\left(p+\frac{2m_c}{E_V+M_V}\Delta\right)\right]\Bigg)\Bigg\}\Psi_{B_c}(\mathbf{p}), \qquad \text{(A.18)}$$

where

$$|\mathbf{\Delta}| = \sqrt{\frac{(M_{B_c}^2+M_V^2-q^2)^2}{4M_{B_c}^2}-M_V^2},$$
$$E_V = \sqrt{M_V^2+\mathbf{\Delta}^2}.$$

[1] CDF Collaboration, F. Abe *et al.*, Phys. Rev. D **58**, 112004 (1998).

[2] I. P. Gouz, V. V. Kiselev, A. K. Likhoded, V. I. Romanovsky, and O. P. Yushchenko, hep-ph/0211432.

[3] V. O. Galkin, A. Yu. Mishurov and R. N. Faustov, Yad. Fiz. **55**, 2175 (1992) [Sov. J. Nucl. Phys. **55**, 1207 (1992)].

[4] D. Ebert, R. N. Faustov and V. O. Galkin, Phys. Rev. D **62**, 034014 (2000).

[5] D. Ebert, V. O. Galkin and R. N. Faustov, Phys. Rev. D **57**, 5663 (1998); **59**, 019902(E) (1999).

[6] V. O. Galkin and R. N. Faustov, Yad. Fiz. **44**, 1575 (1986) [Sov. J. Nucl. Phys. **44**, 1023 (1986)]; D. Ebert, R. N. Faustov and V. O. Galkin, Phys. Lett. B **537**, 241 (2002).

[7] R. N. Faustov and V. O. Galkin, Z. Phys. C **66**, 119 (1995); D. Ebert, R. N. Faustov and V. O. Galkin, Phys. Rev. D **62**, 014032 (2000).

[8] D. Ebert, R. N. Faustov and V. O. Galkin, Phys. Rev. D **56**, 312 (1997); R. N. Faustov, V. O. Galkin and A. Yu. Mishurov, Phys. Rev. D **53**, 6302 (1996); **53**, 1391 (1996).

[9] D. Ebert, R. N. Faustov and V. O. Galkin, Phys. Rev. D **67**, 014027 (2003).

[10] A. A. Logunov and A. N. Tavkhelidze, Nuovo Cimento **29**, 380 (1963).

[11] A. P. Martynenko and R. N. Faustov, Theor. Math. Phys. **64**, 765 (1985) [Teor. Mat. Fiz. **64**, 179 (1985)].

[12] E. Eichten and F. Feinberg, Phys. Rev. D **23**, 2724 (1981).

[13] H. J. Schnitzer, Phys. Rev. D **18**, 3482 (1978).

[14] R. N. Faustov, Ann. Phys. **78**, 176 (1973); Nuovo Cimento A **69**, 37 (1970).

[15] E. Jenkins, M. Luke, A. V. Manohar and M. Savage, Nucl. Phys. B **390**, 463 (1993).

[16] Particle Data Group, K. Hagiwara *et al.*, Phys. Rev. D **66**, 010001 (2002).

[17] M. A. Ivanov, J. G. Körner and P. Santorelli, Phys. Rev. D **63**, 074010 (2001).

[18] V. V. Kiselev, A. K. Likhoded and A. I. Onishchenko, Nucl. Phys. B **569**, 473 (2000); V. V. Kiselev, hep-ph/0211021.

[19] A. Abd El-Hady, J. H. Muñoz and J. P. Vary, Phys. Rev. D **62**, 014019 (2000).

[20] C.-H. Chang and Y.-Q. Chen, Phys. Rev. D **49**, 3399 (1994).

[21] P. Colangelo and F. De Fazio, Phys. Rev. D **61**, 034012 (2000).

[22] A. Yu. Anisimov, P. Yu. Kulikov, I. M. Narodetskii and K. A. Ter-Martirosyan, Phys. Atom. Nucl. **62**, 1739 (1999) [Yad. Fiz. **62**, 1868 (1999)].

[23] M. A. Nobes and R. M. Woloshyn, J. Phys. G **26**, 1079 (2000).
[24] G. Lu, Y. Yang and H. Li, Phys. Lett. B **341**, 391 (1995).
[25] J.-F. Liu and K.-T. Chao, Phys. Rev. D **56**, 4133 (1997).
[26] M. Bauer, B. Stech, and M. Wirbel, Z. Phys. C **34**, 103 (1987).
[27] M. J. Dugan and B. Grinstein, Phys. Lett. B **255**, 583 (1991).
[28] J. D. Bjorken, Nucl. Phys. B (Proc. Suppl.) **11**, 325 (1989).
[29] M. Beneke, G. Buchalla, M. Neubert and C. T. Sachrajda, Phys. Rev. Lett. **83**, 1914 (1999); Nucl. Phys. B **591**, 313 (2000).
[30] A. J. Buras and L. Silvestrini, Nucl. Phys. B **569**, 3 (2000).